Dalton Transactions

ROYAL SOCIETY OF CHEMISTRY

PERSPECTIVE

View Article Online
View Journal | View Issue

Cite this: *Dalton Trans.*, 2026, **55**, 17

MOF/COF-integrated strategies for aqueous zinc batteries: recent progress, modification approaches, and future guidelines

Zihao Jiang,[a] Mingkun Xie,[b] Qingyuan Ma,[c] Peidong Liu[d] and Huaming Yu *[e]

Received 7th October 2025,
Accepted 27th October 2025

DOI: 10.1039/d5dt02398j

rsc.li/dalton

Aqueous zinc-ion batteries (AZIBs) are promising for energy storage, yet challenges like dendrite growth, corrosion, and low coulombic efficiency (CE) hinder their practicality. Metal–organic frameworks (MOFs) and covalent organic frameworks (COFs) have emerged as versatile materials to address these issues due to their designable porous structures, tunable surface properties, and high stability. This review summarizes the cutting-edge advancements of MOFs and COFs in AZIBs, which are mainly divided into two aspects: (1) adjustments to the intrinsic physical structures of MOFs and COFs, such as pore size, functional groups and the metal species in porous frameworks, and (2) modifications to battery components, including separators, cathodes/anodes and electrolytes. From diverse perspectives, these viewpoints propose solutions to the existing challenges in AZIBs, effectively enhancing battery performance. Meanwhile, this article constructs a structure–performance–material logical framework centered on MOFs/COFs for AZIBs and offers viable guidelines for next-generation MOF/COF-integrated energy storage systems.

[a]*Sustainable Energy and Environment Thrust, Function Hub, The Hong Kong University of Science and Technology (Guangzhou), Guangzhou 511400, China*
[b]*Department of Materials Science and Engineering, National University of Singapore, Singapore 117575, Singapore*
[c]*Department of Systems Engineering, City University of Hong Kong, Hong Kong 999077, China*
[d]*Department of Mining and Minerals Engineering, Virginia Polytechnic Institute and State University, Blacksburg, VA, 24061, USA*
[e]*Advanced Materials Thrust, Function Hub, The Hong Kong University of Science and Technology (Guangzhou), Guangzhou 511400, China.*
E-mail: hmYu147@outlook.com, hyu176@connect.hkust-gz.edu.cn

1. Introduction

With the rapid depletion of fossil fuels and the growing global emphasis on sustainable development, renewable energy sources such as geothermal, wind, and solar energy have become crucial pillars of future energy systems.[1,2] However, the inherent intermittency and instability of these renewable energy sources necessitate efficient energy storage technologies to achieve their large-scale application[3–5] Some significant

Zihao Jiang

Zihao Jiang obtained his Bachelor's degree from the Powder Metallurgy Research Institute at Central South University in 2020 and his Master's degree from the School of Emergent Soft Matter at South China University of Technology in 2023. He is currently pursuing a Doctoral degree at The Hong Kong University of Science and Technology (Guangzhou), where his research focuses on crystalline porous materials, particularly concentrating on the applications of metal–organic frameworks and covalent organic frameworks.

Mingkun Xie

Mingkun Xie received his Bachelor's from the Powder Metallurgy Research Institute at Central South University in 2020. He achieved his Master's studies at the National University of Singapore, focusing on energy storage devices and materials, especially for high-performance thermoelectrical materials.

efforts have also been devoted to developing advanced functional materials for energy storage and environmental monitoring.[6–8] Rechargeable batteries, as one of the most mature energy storage technologies, have been widely used in electric vehicles, portable electronics, medical devices, and military equipment.[9–11]

Among various battery systems, aqueous zinc-ion batteries have emerged as promising alternatives to lithium-ion batteries (LIBs) due to their advantages of high safety, low cost, and abundant zinc resources.[12–14] Zn metal has a high theoretical specific capacity (820 mAh g^{-1}) and a suitable redox potential (−0.762 V *vs.* SHE), making it an ideal electrode material.[15,16] However, AZIBs face severe challenges: anodes have dendrite growth, the hydrogen evolution reaction (HER), corrosion, and passivation.[17–20] The growth of Zn dendrites not only increases the impedance of the battery but also exacerbates side reactions by expanding the exposed area of the anode, forming a vicious cycle of dendrite growth-side reactions–further dendrite nucleation.[21,22] In aqueous electrolytes, the thermodynamic instability of Zn metal leads to HER and corrosion, and the generated by-products, such as $Zn_4SO_4(OH)_6{\cdot}xH_2O$, which form a passivation layer on the anode surface, further reduce the coulombic efficiency (CE) and cycle performance.[23] Meanwhile, there are also some problems faced by cathode materials. The repeated insertion and extraction of Zn^{2+} ions during cycling induces significant lattice strain in the cathode material, often leading to particle cracking, structural distortion, or phase transitions. This progressive structural degradation directly compromises cycling stability and shortens the battery's service life. Additionally, certain cathode materials, particularly manganese- and vanadium-based oxides, suffer from issues such as dissolution, oxygen loss, or irreversible side reactions with the electrolyte. These processes consume active material, increase interfacial impedance, and result in notable capacity fading over time. The structural instability and interfacial side reactions further hinder the smooth migration of Zn^{2+}, increase electrode polarization, and reduce energy efficiency during charge–discharge cycles, manifesting as low CE.[24,25]

To address these challenges, researchers have developed various strategies, including electrolyte optimization, electrode structure design, and interface modification.[26–29] Among them, the application of porous framework materials represented by metal–organic frameworks (MOFs) and covalent organic frameworks (COFs) has shown great potential. MOFs are porous crystalline materials formed by the coordination of metal ions/clusters and organic ligands, featuring controllable topological structures, large specific surface areas, and high thermal stability.[30–32] COFs are crystalline porous polymers constructed by covalent bonding of organic building units, with adjustable pore structures, abundant active sites, and excellent chemical stability.[33–35] Both MOFs and COFs possess designable porous structures, tunable surface properties, and high stability, which enable them to regulate ion transport, inhibit dendrite growth, and improve interface stability in Zn batteries (Fig. 1).[36,37]

Specifically, MOFs and COFs can optimize battery performance through two main approaches: intrinsic structure adjustment and battery component modification. In terms of intrinsic structure adjustment, the pore size, functional groups, and metal species in the frameworks can be precisely regulated to achieve selective ion transport and uniform ion deposition.[38–40] For component modification, MOFs and COFs can be applied to separators, cathodes/anodes, and electrolytes to enhance ion conductivity, inhibit side reactions, and improve the stability of electrode materials.[41–43] These strategies provide effective solutions to the existing challenges in AZIBs from multiple perspectives, significantly enhancing battery performance. This review systematically summarizes the cutting-edge advancements of MOFs and COFs in AZIBs. By constructing a structure–performance–material logical framework centered on MOFs/COFs (Fig. 2a), it aims to clarify the intrinsic relationship between the rational design of MOF/COF structures and their working mechanisms in batteries. Based on their unique advantages, the application and research of MOFs/COFs in AZIBs have been rapidly expanding over the past decade, leading to a significant increase in the number of related publications (Fig. 2b). Finally, this review

Qingyuan Ma

Qingyuan Ma obtained his B.Eng. and M.Eng. degrees from the Powder Metallurgy Research Institute at Central South University in 2020 and 2023, respectively. He is currently pursuing a Ph.D. degree at the City University of Hong Kong. His research interests lie in the field of dynamic laser manufacturing driven by beam shaping techniques including additive and subtractive manufacturing.

Peidong Liu

Peidong Liu received his Bachelor's and Master's degrees at Central South University and is currently pursuing his doctoral studies at Virginia Polytechnic Institute and State University. His research centers on sustainable valorization of waste streams through interdisciplinary techniques, especially for critical mineral recovery from industrial wastewater, to advance scalable, cost-effective, and environmentally responsible solutions.

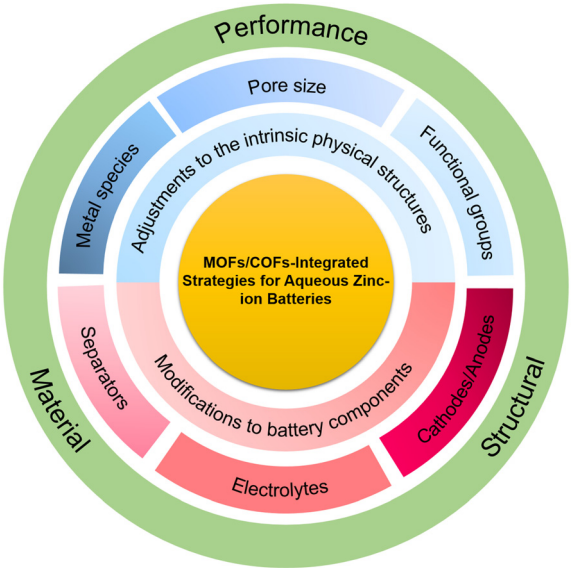

Fig. 1 MOF/COF-integrated strategies for AZIBs.

offers viable guidelines for the development of next-generation MOF/COF-integrated energy storage systems, promoting the practical application of high-performance Zn batteries.

2. Mechanisms of MOFs/COFs in improving the stability of AZIBs

MOFs and COFs can enhance battery stability and performance primarily by suppressing dendrite growth and interfacial side reactions for anodes; and inhibiting volume expansion and structural collapse for cathodes. Their well-defined porous structures regulate ion flux to ensure uniform metal plating, thereby preventing dendrite initiation. Simultaneously, their tunable functional groups can sequester harmful reactants or form a protective layer, effectively passivating the electrode interface against parasitic chemical degradation.

Huaming Yu

Huaming Yu received his Bachelor's and Master's degrees from the Powder Metallurgy Research Institute at Central South University in 2020 and 2023, respectively. He is currently pursuing his doctoral studies at The Hong Kong University of Science and Technology (Guangzhou), focusing on low cost and environmental energy storage devices, especially for high-performance metal batteries and rational design of thermocells.

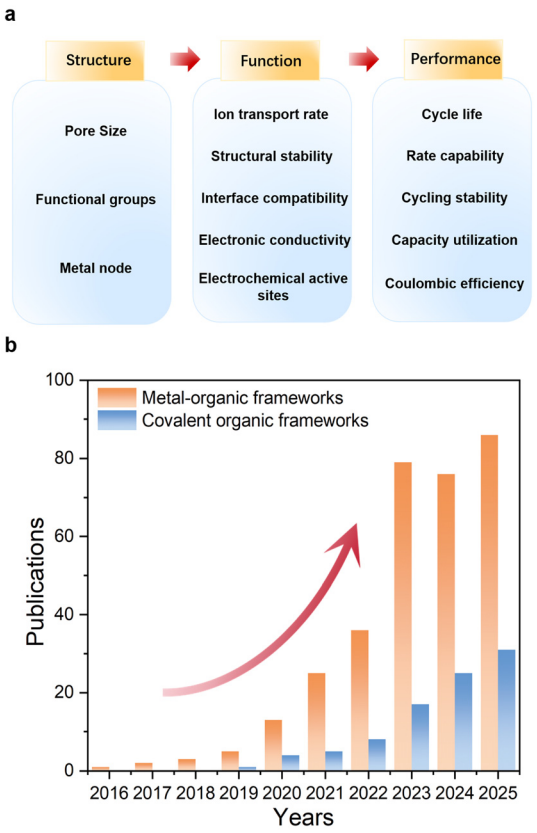

Fig. 2 (a) Schematic of the logical statement for MOFs/COFs on the structure–performance–material framework. (b) Publication of applications and research on MOFs/COFs in AZIBs for recent decades.

Benefiting from the controllable assembly characteristics of metal clusters/nodes and organic ligands, MOFs can address the dendrite growth issue of Zn metal anodes through multi-dimensional synergistic effects. Their core logic starts from the dual pathways of inhibiting the uneven deposition of Zn^{2+} and blocking the interfacial side reaction during cycling. MOFs further leverage their porous structure, zincophilic sites, mechanical stability, and interface regulation capabilities to construct an integrated protection–regulation system which is suitable for the electrochemical environment of AZIBs. Similarly, COFs, endowed with designable porous structures, tunable surface properties, and stable chemical characteristics, also tackle the different problems on AZIBs *via* a synergistic approach, while additionally exhibiting differentiated action pathways in response to the distinct electrochemical properties of AZIBs. More importantly, the highly crystalline π-conjugated structure of covalent organic frameworks can provide a stable physical and chemical reaction environment, which is particularly beneficial for achieving excellent electrochemical stability.[9]

2.1. Mechanisms of inhibiting dendrite growth

When all the discharge products of zinc on the anode have decreased, the zincate in the electrolyte on the surface of the zinc-based anode begins to be reduced, thereby plating metal-

lic zinc. When the zinc ore near the anode surface is consumed, most of the zinc ore is located outside the electrolyte or inside the separator, rather than on the surface of the porous zinc electrode.[44] This phenomenon leads to severe concentration polarization. This uneven distribution of zinc ions can thereby control the deposition process of zinc. Therefore, Zn^{2+} are more likely to migrate to the tips of the electrode surface protrusions rather than reach other domains.[45]

The inhomogeneity of the surface morphology of Zn metal anodes can easily lead to the formation of dendrites. This unevenness is caused by the free diffusion of zinc ions on the electrode surface. The free movement of zinc ions makes it easy for them to migrate to energy-favorable sites for charge transfer. Therefore, the aggregation of zinc ions is prone to occur and eventually becomes the nucleation site of zinc dendrites. Here are some mechanisms of common methods for inhibiting dendrite growth.[46]

2.1.1. Regulating metal ion flux *via* ordered pores. The root cause of Zn dendrite growth is the tip effect: the local concentration imbalance and disordered diffusion of Zn^{2+}, during charging, means Zn^{2+} tends to accumulate at protrusions on the electrode surface, leading to preferential deposition and dendrite formation. The long-range ordered nanochannels of MOFs and COFs can act as Zn^{2+} guided transporters. Through pore size matching and channel directionality constraints, Zn^{2+} is forced to migrate along uniform paths, avoiding excessive local flux and fundamentally inhibiting dendrite nucleation (Fig. 3a).[47]

For MOFs, the pore size of the MOFs can be precisely adjusted by selecting the length of the organic ligands or the type of metal cluster (usually 0.8–12 Å), and it needs to be slightly larger than the diameter of hydrated Zn^{2+} ions (~4.0 Å). This ensures the smooth transport of Zn^{2+} while preventing the penetration of anions that trigger side reactions (Fig. 3b).[48] Take the defective MOF nanoparticle D-UiO-66 as an example. D-UiO-66 is a derivative of UiO-66 obtained through pore size modification. Using D-UiO-66 and zinc salt electrolyte to form the quasi-solid interface, the positively charged defects in D-UiO-66 fixed the anions in the electrolyte through Lewis acid–base interaction. This immobilization not only hinders the migration of anions but also forms anion-modified MOF channels to facilitate the transport of Zn^{2+}, ultimately increasing the cation transference number. In addition, the liquid phase between the channels endows this layer with high ionic conductivity. It is worth noting that due to the partial desolvation within the porous layer, the electrolyte in the quasi-solid interface layer is in a highly concentrated state, making it act as a zinc ion reservoir, which alleviates concentration polarization and enables uniform distribution of zinc ions.[48]

For COFs, pore size regulation follows a similar fundamental logic but requires optimization tailored to different metal anodes. Specifically, Wu *et al.* reported that they designed and *in situ* synthesized an ultrathin, uniform, and mechanically robust three-dimensional COOH-functionalized COF film (3D-COOH–COF) to serve as a protective layer for Zn anodes. This rationally constructed 3D-COOH–COF protective layer confers multiple synergistic advantages for Zn anode stabilization: its ultrathin thickness and well-defined, homogeneous nanochannels enable rapid and uniform diffusion of Zn^{2+} across the Zn anode surface, addressing the issue of sluggish ion transfer at the electrode–electrolyte interface; the abundant negatively charged COOH functional groups anchored on the 3D COF skeleton, coupled with the size confinement effect of its nanochannels, effectively impede the permeation of SO_4^{2-}, which not only enhances the Zn^{2+} transference number but also fundamentally suppresses the heterogeneous nucleation of Zn dendrites; the 3D-COOH–COF film fully and seamlessly covers the Zn anode and current collector, eliminating interfacial gaps and thus blocking direct contact between the Zn metal and aqueous electrolyte, significantly inhibiting parasitic corrosion reactions that degrade anode performance. These merits enable the 3D-COOH–COF layer to simultaneously reduce side reactions *via* selective acceleration of Zn^{2+} transport and inhibition of anion permeation and by ensuring uniform Zn^{2+} plating/stripping to suppress dendrite growth (Fig. 3c). As a result, batteries assembled with 3D-COOH–COF-protected Zn anodes deliver excellent electrochemical performance, with COFs having ~1.0–1.3 nm pores restricting the unconstrained 2D diffusion of Zn^{2+}, guiding directional deposition *via* pore functional groups and avoiding dendrite nucleation at electrode defects.[49]

2.1.2. Inducing uniform nucleation *via* metal-philic sites. Dendrite formation is further driven by the preferential nucleation of metal ions at high-energy sites. MOFs and COFs introduce zincophilic sites to reduce nucleation barriers and guide horizontal deposition on low-energy crystal planes, replacing the tip-preferential growth mode.

MOFs rely on both metal nodes and surface functional groups to create zincophilic sites. Metal nodes anchor metal ions *via* Lewis acid–base interactions, providing stable nucleation sites; functional groups such as –COOH, $-SO_3H$, or ethylene diamine tetraacetic acid (EDTA) further enhance metal affinity.[54] For example, UiO-66–$(COOH)_2$ reduces the Zn nucleation overpotential from 48.3 mV for bare Zn to 20.2 mV *via* –COOH coordination with Zn^{2+}, while EDTA-grafted MOF-808/MOF-E forms five-membered rings with Zn^{2+} to guide (002) plane deposition (Fig. 3d).[50,55]

COFs achieve similar effects through heteroatoms or polar functional groups, with customizable frameworks enabling precise regulation of Zn anode deposition. For Zn anodes, $-SO_3H$ or C=N groups act as zincophilic sites and synergize with ordered pores to guide deposition. Take TpPa–SO_3H COF an as example; *via* liquid–liquid interface synthesis, it forms a uniform film on Zn foil. Its $-SO_3H$ groups strongly adsorb Zn^{2+} to lower the nucleation overpotential, and release H^+ to inhibit by-products like $Zn_4SO_4(OH)_6{\cdot}xH_2O$ (Fig. 3e).[51] Electrochemically, a TpPa–SO_3H@Zn//Cu asymmetric cell reached a high coulombic efficiency of >99% over 1000 cycles, and symmetric cell cycles stably >600 h, far outperforming the bare Zn anode.[51]

2.1.3. Constructing physical barriers. When dendrites grow to a critical size, they pierce the separator and cause short circuits. MOFs and COFs leverage their mechanical strength and

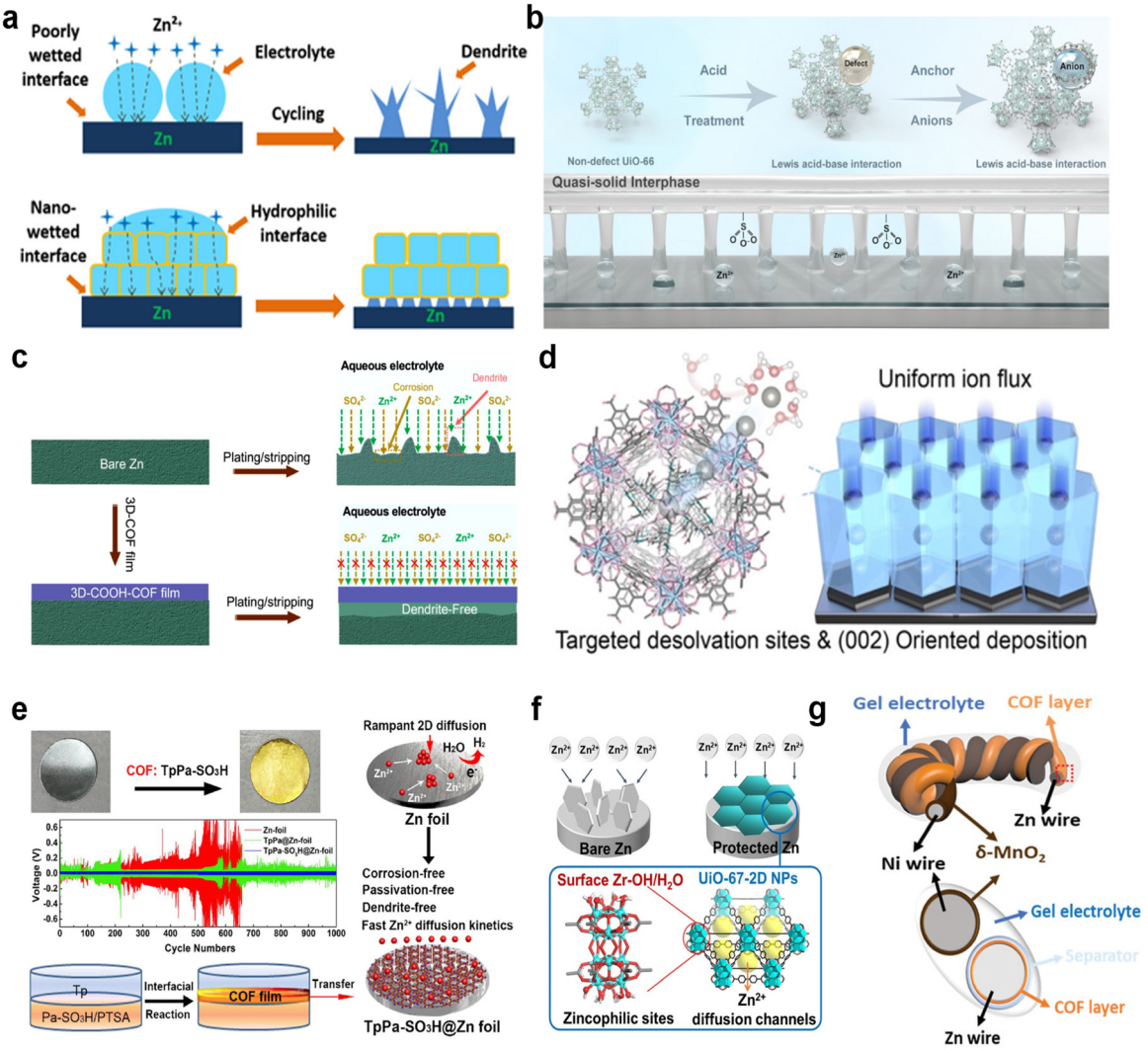

Fig. 3 Strategies in inhibiting dendrite growth for AZIBs. (a) Using MOFs to form the layer to improve the wetting effect of the aqueous electrolyte on the zinc anode. Reproduced with permission from ref. 47 Copyright 2019, American Chemical Society. (b) Adjusting the pore size of MOFs to prevent side reactions in AZIBs. Reproduced with permission from ref. 48 Copyright 2023, Springer Nature. (c) Schematic illustration of the Zn deposition behavior on the bare Zn and 3D-COOH COF@Zn. Reproduced with permission from ref. 49 Copyright 2022, Elsevier. (d) Cage-channel structure of 3D MOFs. Reproduced with permission from ref. 50 Copyright 2023, Wiley-VCH. (e) TpPa–SO_3H films are fabricated and coated on Zn metal to stabilize the anode. Reproduced with permission from ref. 51 Copyright 2022, Elsevier. (f) UiO-67-based MOF films on Zn anodes compared with bare zinc. Reproduced with permission from ref. 52 Copyright 2022, Springer Nature. (g) The DIP-D COF film with a high Young's modulus in zinc electrolyte. Reproduced with permission from ref. 53 Copyright 2021, Wiley-VCH.

structural flexibility to form "physical barriers" that block dendrite extension and adapt to electrode volume changes. For Zn anodes, the higher hardness of Zn makes dendrites more likely to penetrate separators, so the physical barrier needs to balance puncture resistance and flexibility. MOFs and COFs can form a continuous protective layer on the Zn surface, not only physically blocking dendrite growth but also buffering the volume expansion during Zn plating/stripping, avoiding the formation of new cracks that provide sites for dendrite nucleation.[56] This dual effect of blocking and buffering is crucial for solving the dendrite problem of Zn anodes.

MOFs with high mechanical stability rely on strong metal–ligand bonds to resist dendrite puncture. 2D MOF nanosheets form crack-free dense coatings on Zn surfaces, wrapping electrode protrusions to prevent local Zn^{2+} over-deposition.[48,52] The dense structure of 2D MOF nanosheets can avoid electrolyte penetration, reducing side reactions like hydrogen evolution. For example, UiO-67-based MOF films on Zn anodes can reduce the corrosion current density by 37% compared with bare Zn, while their high mechanical modulus (over 5 GPa) ensures that even when Zn dendrites start to grow, they cannot pierce the MOF layer, thus avoiding short circuits (Fig. 3f).[56]

COFs balance rigidity and flexibility for different anodes. For Zn anodes, ultra-thin flexible COF films avoid rupture during volume expansion while maintaining anti-penetration

capability These films achieve low interfacial impedance while blocking dendrite penetration.[53,57] For instance, the DIP-D COF film has a Young's modulus of 0.1–0.2 GPa, which can adapt to the volume change of Zn anodes without cracking. Meanwhile, its ordered nanochannels ensure that the interfacial impedance does not increase significantly. In symmetric cell tests, DIP-D COF@Zn symmetric cells can cycle stably for over 300 h at 1 mA cm^{-2} and 1 mAh cm^{-2}, while the bare Zn cell presents an obvious short circuit only after ~14 h, confirming the excellent physical barrier effect of COF films (Fig. 3g).[53]

2.2. Mechanisms of suppressing interfacial side reactions

2.2.1. Constructing stable artificial SEI layers. Unstable solid electrolyte interphase (SEI) layers or passivation layers exacerbate side reactions and dendrite growth for Zn anodes. The naturally formed SEI on Zn is usually porous and uneven, easily cracking during plating/stripping, which exposes fresh Zn to the electrolyte, triggering continuous HER and corrosion. MOFs and COFs, with their ordered porous structures and tunable functional groups, act as artificial interface layers to stabilize these films and reduce electrolyte decomposition—they not only block direct contact between the Zn and electrolyte but also regulate ion transport to avoid uneven SEI regeneration.[56]

On Zn metal anodes, MOFs/COFs do not form traditional SEIs but construct ion-selective passivation layers. For example, sulfonated MOFs or COFs form a Zn^{2+}-conductive layer.[51] The $-SO_3H$ groups strongly coordinate with Zn^{2+}, guiding uniform Zn deposition while repelling SO_4^{2-} to suppress the formation of by-products. COFs' ordered nanochannels of about 1.2 nm further homogenize Zn^{2+} flux, maintaining a stable interface during cycling.[39,58]

For Zn anodes, $-SO_3H$ or C=N groups act as zincophilic sites and synergize with ordered pores to guide deposition. Take TpPa–SO_3H COF as an example; *via* liquid–liquid interface synthesis, it forms a uniform film on Zn foil. Its $-SO_3H$ groups strongly adsorb Zn^{2+} (adsorption energy −1.97 eV) to lower the nucleation overpotential, and release H^+ to inhibit by-products like $Zn_4SO_4(OH)_6{\cdot}xH_2O$.

2.2.2. Isolating the electrolyte contact. Direct contact between electrodes and electrolytes triggers severe side reactions, including the HER and corrosion in aqueous systems. These reactions not only consume active Zn and electrolytes but also generate inert by-products which increase interfacial impedance, creating a vicious cycle with dendrite growth. MOFs and COFs can address this by constructing physical or chemical barriers to block direct electrode–electrolyte contact, relying on their dense porous structures or hydrophobic modification to reduce parasitic reactions.[59]

For MOFs, hydrophobic surface engineering is a key strategy to inhibit water penetration. For example, ZIF-7, a zeolitic imidazolate framework, has a water contact angle of ~135° due to its methyl-substituted imidazole ligands. This strong hydrophobicity forms a "saturated electrolyte interphase" on the Zn surface, preventing H_2O molecules from reaching the Zn anode. Tests show the HER rate of ZIF-7-modified Zn is only 0.02 mL h^{-1}, 1/15 that of bare Zn, and symmetric cells with ZIF-7@Zn can cycle stably for 3000 h at 0.5 mA cm^{-2} (Fig. 4a).[60] Similarly, ZIF-8 can be modified *via* a vapor–solid reaction to form a seamless 0.7 μm-thick layer with molecule-sieving properties, blocking electrolyte infiltration while maintaining Zn^{2+} transport channels.[59] Additionally, HKUST-1, an organophilic MOF, can trap organic electrolytes in its pores to form a phase-separated interface, isolating the Zn anode from aqueous electrolytes and suppressing corrosion effectively (Fig. 4b).[61]

COFs isolate electrolytes through functional group modification or structural design. Fluorinated COFs (*e.g.*, F-CTFs with 0.5 nm ultramicropores) use electronegative fluorine atoms to repel water molecules, reducing the HER by limiting H_2O access to Zn. Alkynyl-rich flower-like COF–H, with a water contact angle of 141°, forms a dense hydrophobic coating. After 900 cycles at 3 mA cm^{-2}, no corrosion products are detected on the Zn surface, and the CE remains above 99.2% (Fig. 4c).[62,63]

2.2.3. Regulating the local interface pH. HER on Zn anodes consumes H^+ and increases local OH^- concentration, disrupting the interface pH balance. The elevated OH^- reacts with Zn^{2+} and electrolyte anions to form by-products which accumulate as inert layers to worsen ion transport and induce uneven Zn deposition.[65] MOFs/COFs can regulate local pH *via* acidic functional groups, neutralizing excess OH^- to inhibit HER and maintain interface uniformity.

Some specific MOFs with –COOH or $-SO_3H$ groups such as UiO-66–$(COOH)_2$ and TpPa–SO_3H MOF can release H^+ to neutralize OH^-, maintaining the local pH at 4.0–5.0. This reduces the HER rate by 70% and prevents the formation of $Zn_4SO_4(OH)_6{\cdot}xH_2O$, as confirmed by XPS.[51,55] UiO-66–$(COOH)_2$, has been developed as the multifunctional ion-conductive interphase to stabilize the Zn anode. The strong interaction between the carboxyl groups within UiO-66–$(COOH)_2$ and hydrated Zn^{2+} could construct a concentrated electrolyte in the channels, promote the diffusion of electrolyte, and facilitate the desolvation of hydrated Zn^{2+}, thereby inhibiting the water-induced side reactions and dendrite growth.

COFs use similar acid–base regulation. $-SO_3H$-functionalized TpPa–SO_3H COF releases H^+ to counteract HER-generated OH^-. COOH-functionalized 3D COFs maintain local pH stability, with their uniform nanochannels homogenizing Zn^{2+} flux. Additionally, density functional theory (DFT) calculations show it reduces the Zn^{2+} desolvation energy from 52.95 to 23.21 kJ mol^{-1}, accelerating ion transport. A symmetric cell with COF@Zn exhibits over 2000 h of stable cycling, and the surface of electrode shows no by-product accumulation after cycling, confirming effective pH regulation.[59]

2.3. Mechanisms of inhibiting volume expansion and structural collapse

So far, research has been conducted on a library of inorganic cathode materials such as manganese-based oxides

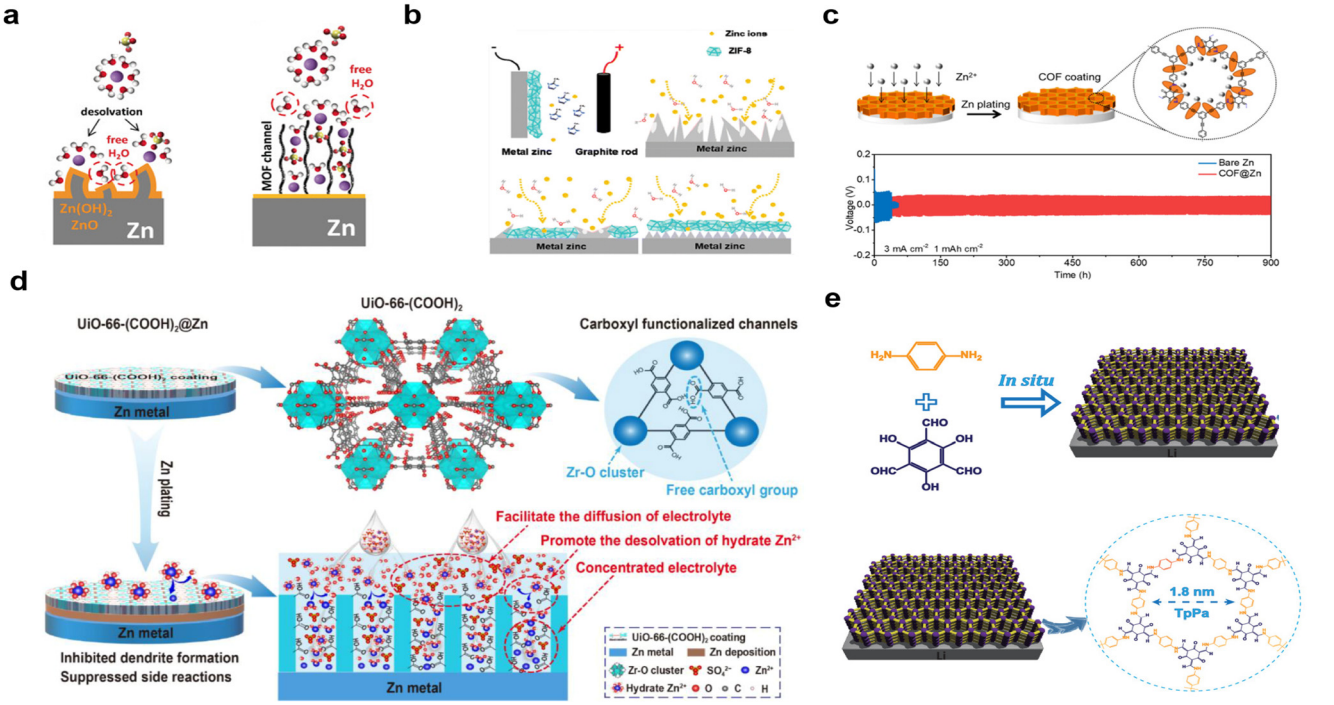

Fig. 4 COFs' strategies in isolating the electrolyte contact for AZIBs. (a) Schematic illustration of the surface evolution of Zn. Reproduced with permission from ref. 60 Copyright 2020, Wiley-VCH. (b) Schematic of electrodeposition of ZIF-8 on Zn. Reproduced with permission from ref. 62 Copyright 2021, Wiley-VCH. (c) Schematic illustrations of Zn plating on bare Zn and COF@Zn electrodes and the cycling performance of COF@Zn and bare Zn-based symmetrical batteries. Reproduced with permission from ref. 63 Copyright 2022, American Chemical Society. (d) Schematic illustration of the functional mechanism of the UiO-66–$(COOH)_2$ coating layer for protecting the Zn anode. Reproduced with permission from ref. 55 Copyright 2023, Elsevier. (e) Reaction scheme of TpPa from Tp and Pa. Reproduced with permission from ref. 64. Copyright 2021, Wiley-VCH.

and vanadium-based oxides, which exhibit high capacity in AZIBs.[66–68] However, during the zinc-ion intercalation process, inorganic materials undergo significant volume expansion and structural collapse due to volume structural stress and irreversible dissolution, which reduces capacity output and cycling stability.[69] In recent years, various organic materials such as carbonyl compounds and imine compounds have been regarded as highly promising next-generation cathode materials in zinc-ion batteries due to their advantage of electrochemical reversibility. Nevertheless, most active molecules and low molecular weight compounds are poor-performing electrode materials in zinc-ion batteries due to low conductivity and unavoidable solubility issues.

The combination of various transition metal ions or metal clusters with different organic ligands endows MOFs with high specific surface area and significant porosity. Their abundant pore structures provide sufficient Zn^{2+} storage sites during electrochemical processes. Currently, the zinc storage mechanisms of MOF-based cathode materials mainly include the insertion/extraction of Zn^{2+}, or the co-insertion/co-extraction mechanism of H^+ and Zn^{2+}. MOFs mainly achieve Zn^{2+} storage through reactions between Zn^{2+} and C═O or C═N bonds in their organic ligands, thereby providing capacity for batteries.[24] In addition, transition metal ions or metal clusters in some MOFs can further improve capacity through redox reactions during electrochemical processes. By combining the porous framework of MOFs, the high conductivity of derived carbon, and the high activity of traditional cathode materials, MOF derivatives exhibit excellent conductivity and outstanding rate performance. The zinc storage mechanisms of MOFs and their derivatives are usually determined by factors such as the structure of the cathode material and the type of electrolyte used. Therefore, understanding the zinc storage mechanisms of different materials is crucial for improving the capacity and cycling stability of MOF-based cathode materials in AZIBs.

As an emerging crystalline and porous polymer material, COF exhibits high chemical stability, good porosity, and the ability to design redox-active groups within its framework. These characteristics enable COFs to be widely used as electrode materials in rechargeable batteries.[24] Compared with traditional amorphous organic polymers, COFs can achieve the directional assembly of redox-active sites, thereby realizing specific spatial structures and redox properties. The storage mechanism of COFs is similar to that of organic molecules in aqueous electrolyte, where Zn^{2+} or H^+ undergoes reversible coordination and dissociation with functional groups in the COF structure. Redox-active functional groups are mainly based on units containing C═O, C═N, or N═N, while other

bonds lacking redox-active sites are mainly used to construct the spatial framework.[9] Compared with the dissolution problem associated with traditional metal oxides, COF has a covalent structure with stronger chemical bonds, making it more suitable for manufacturing stable cathode materials. In addition, strategies such as introducing redox-active groups and optimizing the pore structure to improve the utilization of active sites are expected to obtain COF cathode materials with better performance.[70] Although research is still in the early stage, there is still much room for development.

2.4. Mechanism synergy

In practical applications, MOFs and COFs do not rely on a single mechanism but achieve optimal dendrite inhibition and interface stabilization through the synergistic coupling of the above effects. The multi-dimensional synergy of MOFs/COFs, integrating ion flux regulation, nucleation induction, a physical barrier, and interface passivation, is their core advantage over traditional organic or inorganic coatings.[57,64,71] It is worth noting that the defective grain boundaries in these polycrystalline MOFs/COFs can also function through defects, voids, or amorphous domains effect. Table 1 lists several common mechanisms of MOFs and COFs in synergistic effects. Due to space limitations, only the representative MOFs/COFs among them are introduced.

For MOFs, UiO-66–$(COOH)_2$ exemplifies this synergy: its 8 Å pores match the hydrated Zn^{2+} diameter to homogenize ion flux, –COOH groups as zincophilic sites can reduce Zn nucleation overpotential to guide uniform deposition, and $Zr_6O_6(OH)_6$ clusters with the strong Zr–O bonds of about 600 kJ mol^{-1} can maintain structural stability in aqueous electrolytes—enabling Zn anodes to cycle stably for 2800 h at 2 mA cm^{-2} (Fig. 4d).[55] Similarly, EDTA-grafted MOF-808/MOF-E combines 3D interconnected pores to achieve flux regulation, using EDTA's Zn^{2+} chelation to guide nucleation, and using Zr^{4+} nodes to improve the corrosion resistance can then achieve dendrite-free Zn deposition even at high capacity of 5 mAh cm^{-2}, with symmetric cells showing no voltage fluctuation for 900 h.[50]

Many MOF materials have problems such as poor electrical conductivity and insufficient stability. COFs, as a crystalline and porous polymer material, have a covalent structure and stronger chemical bonds, thus featuring high chemical stability, good porosity, and the ability to design REDOX active groups within its framework. Some scientific research teams use TAPB–PDA COF to achieve synergistic coupling of dimensional effects by COFs: TAPB–PDA COF uses N atoms to achieve nucleation induction, hydrophobic surfaces, and longitudinal pores for ion transport to achieve dendrite-free growth under 5 mAh cm^{-2} (Fig. 4e).[64] The inhibition of dendrites by COFs is achieved by the synergistic coupling of "pore regulation–nucleation induction–interface stabilization".

This synergy not only enhances the individual performance of each mechanism but also addresses trade-offs of high mechanical strength *vs.* low impedance, and ion selectivity *vs.* transport efficiency. In practical applications, traditional materials only address single challenges: many organic polymers lack ion selectivity and zincophilic sites, failing to guide uniform Zn deposition; inorganic modified layers are brittle and easy to crack during volume changes, losing protective effects. In contrast, this synergy enables MOFs/COFs to avoid such trade-offs, becoming the key to their excellent Zn anode protection.[48] It also underpins both MOFs and COFs in achieving an ultra-long cycle life and high coulombic efficiency in AZIBs, Ultimately, this synergy provides a universal design principle for developing high-performance framework materials tailored for stable AZIBs.[47]

3. Adjustments to the intrinsic physical structures of MOFs and COFs

As core porous framework materials for optimizing battery performance, MOFs and COFs possess a unique "modular assembly" feature—their intrinsic physical structures, including pore architecture, surface chemical properties, and metal node composition, can be precisely regulated to match the electrochemical demands of AZIBs. This structural tunability not only enables them to address the root causes of AZIB failure but also lays the foundation for constructing a "structure–performance" correlation that guides material design. Among the two, MOFs, with their metal cluster–organic ligand coordination system, exhibit more flexible adjustability in terms of pore topology, surface functional groups diversity, and metal node stability—making them a research focus in the field of AZIB protection. The following section will first systematically elaborate on the adjustment strategies for the intrinsic physical structures of MOFs, analyzing how modifications to key structural dimensions including pore size/topology, surface functional groups, and metal nodes can synergistically enhance the performance of AZIBs, and will then extend to the structural regulation principles of COFs for a comparative discussion.

Table 1 Common mechanisms of MOFs and COFs in synergistic effects

Ref.	MOF/COF name	Synergistic mechanisms
55	UiO-66–$(COOH)_2$	Ion flux regulation, nucleation induction, structural stability support
50	MOF-808	Flux regulation, nucleation guidance, corrosion resistance
59	ZIF-8	Ion flux regulation, interface stabilization, reduction of nucleation overpotential
64	TAPB–PDA COF	Local pH regulation, nucleation induction, accelerated ion transport
53	DIP-D COF	Physical barrier, low-impedance ion transport, interface corrosion inhibition
49	3D-COOH–COF	Interface stability enhancement, ion sieving and flux homogenization, physical barrier and volume buffering

3.1. Adjustments to the intrinsic physical structures of MOFs

Metal–organic frameworks exhibit unique "metal cluster/organic ligand" modular assembly characteristics, enabling precise regulation of their intrinsic physical structures to match the electrochemical demands of Zn metal anodes. The core of such adjustments lies in optimizing three key structural dimensions—pore size and pore topology, surface functional groups, and metal node species—to achieve "selective ion transport, enhanced zinc affinity, and improved environmental stability". These structural modifications directly address the root causes of AZIB failure: uneven Zn^{2+} deposition, side reactions, and coating degradation, forming a clear "structure–performance" correlation. Below is a detailed analysis of the strategies and mechanisms for each dimension.

3.1.1. Pore size and pore topology regulation. The pore structure of MOFs include pore size, shape, and dimensionality. These figures determine the efficiency and uniformity of Zn^{2+} transport—an essential factor in inhibiting the "tip effect" and dendrite nucleation. The primary regulatory goals are: matching the pore size to the hydrated Zn^{2+} diameter (~4.0 Å) to ensure unobstructed ion transmission while blocking interfering anions; and designing pore topology (2D/3D, channel/cage) to constrain Zn^{2+} diffusion paths and avoid local concentration imbalances.[47,48,50]

Pore size is primarily regulated by selecting organic ligands of different lengths or adjusting the coordination mode of metal clusters. For Zn-ion battery applications, the optimal MOF pore size ranges from 0.8–12 Å—sufficiently large to accommodate hydrated Zn^{2+} but small enough to exclude anions and suppress solvent molecule penetration. For low-current scenarios, short-linker MOFs are preferred; for example, UiO-66 constructed from Zr^{4+} clusters and 1,4-benzenedicarboxylate (BDC) ligands has a dual-pore structure: octahedral central cages (8 Å) and tetrahedral corner cages (6 Å) (Fig. 5a).[72] This pore size matches the hydrated Zn^{2+} diameter, allowing Zn^{2+} to diffuse through the channels with a flux deviation of less than 5%. In another research study, ZIF-8 with the pore size of 18 Å allows SO_4^{2-} to enter the channels, triggering the formation of $Zn_4SO_4(OH)_6{\cdot}xH_2O$ by-products and reducing the CE to <80% after 100 cycles (Fig. 5b and c).[58,73] Thus, pore size matching to hydrated Zn^{2+} is a critical design criterion.

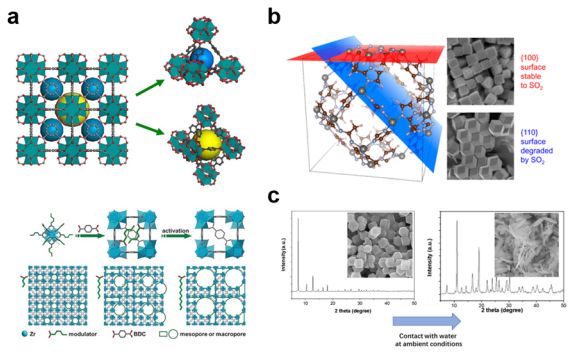

Fig. 5 (a) Schematic illustration of UiO-66 and the synthesis of HP-MOFs with adjustable porosity using UiO-66. Reproduced with permission from ref. 72 Copyright 2024, Elsevier. (b) Schematic of the (110) and (100) crystallographic facets of ZIF-8 under mildly acidic conditions. Reproduced with permission from ref. 58 Copyright 2016, American Chemical Society. (c) Schematic illustrations of ZIF-8 surface change through the water environment. Reproduced with permission from ref. 73 Copyright 2019, Elsevier.

3.1.2. Surface functional group regulation. The surface chemistry of MOFs is predominantly governed by organic ligands. Consequently, functionalizing these ligands to incorporate zincophilic sites or side reaction inhibitors stands as a pivotal strategy for enhancing the performance of AZIBs. The underlying core logic of this approach is threefold: first, introducing polar functional groups enables the formation of coordination bonds with Zn^{2+} ions, which effectively lowers the nucleation barrier during Zn deposition. At the same time, it slows down the collapse rate of the zinc cathode; second, modifying acidic or basic groups allows regulation of the local interfacial pH, thereby suppressing the HER; third, grafting hydrophobic groups creates a barrier to block electrolyte penetration, mitigating the corrosion of the Zn anode and extending its cycle life.

Zincophilic groups (*e.g.*, –COOH, $-SO_3H$, $-NH_2$, EDTA) interact with Zn^{2+} *via* Lewis acid–base coordination or electrostatic attraction, anchoring Zn^{2+} to low-energy sites and avoiding preferential deposition at protrusions. Among these, carboxyl groups (–COOH) exhibit strong coordination with Zn^{2+} (bond energy ~1.8 eV) and improve the hydrophilicity of MOFs for efficient ion transport. Xin *et al.*[55] synthesized UiO-66–$(COOH)_2$ by replacing BDC ligands with 2,5-dicarboxylic acid terephthalate; the –COOH groups on the pore walls reduced the Zn nucleation overpotential from 48.3 mV to 20.2 mV. The modified Zn anode cycled for 2800 h at 2 mA cm^{-2} and 2 mAh cm^{-2}, with an overpotential fluctuation of <10 mV—far superior to unmodified UiO-66. Sulfonic acid groups not only coordinate with Zn^{2+} but also release H^+ to neutralize OH^- generated by the HER, maintaining a stable local pH 4.0–5.0.

Modulating the hydrophilicity of MOF surfaces can reduce direct contact between Zn and aqueous electrolytes, inhibiting corrosion and the HER. For aqueous electrolyte isolation, hydrophobic modification is a key strategy: Yang *et al.*[60] synthesized ZIF-7 which combines Zn^{2+} and benzimidazole ligands with a hydrophobic surface with a water contact angle of 135°. The hydrophobic pores prevented H_2O molecules from reaching the Zn surface, reducing the HER rate to 0.02 mL h^{-1}. The ZIF-7-coated Zn anode cycled for 3000 h at 0.5 mA cm^{-2}, with no corrosion products detected by XPS. For MOFs used as ion-conductive interlayers, hydrophilic groups improve electrolyte wettability. Also, as we mentioned earlier, Liu *et al.*[47] found that UiO-66 with surface hydroxyl groups exhibited a contact angle of 25° with aqueous electrolytes, compared with 60° for hydrophobic ZIF-8. This enhanced wettability reduced the charge-transfer resistance by 30%, enabling faster Zn^{2+} transport.

3.1.3. Metal node regulation. The metal nodes of MOFs, which includes metal ions or clusters, determine their chemi-

cal stability and zinc affinity—critical for long-term cycling in acidic aqueous electrolytes. Regulation strategies focus on selecting high-valence, redox-inert metals to enhance framework stability and optimizing metal cluster structures to expose more zincophilic sites.

According to Pearson's hard and soft acids and bases (HSAB) principle, high-valence metal ions (*e.g.*, Zr^{4+}, Ti^{4+}, Al^{3+}, hard acids) form strong coordination bonds with oxygen-containing ligands, improving MOF stability in aqueous electrolytes. In contrast, low-valence metals such as Zn^{2+} and Cu^{2+} tend to dissociate in acidic environments, leading to framework collapse. For UiO series Zr^{4+}-based MOFs, UiO-66 and UiO-67 use $Zr_6O_4(OH)_4$ clusters as nodes; the Zr–O bond energy is much higher than the Zn–N bond energy in ZIF-8.[74] Xu *et al.*[48] demonstrated that defect-rich UiO-66 (D-UiO-66) retained 90% of its crystalline structure after 1800 cycles in 2 M $ZnSO_4$ electrolyte, whereas ZIF-8 decomposed completely after 1200 cycles and XRD peaks disappeared. Ti-based MOFs exhibit similar stability to Zr-based MOFs and have additional redox activity. Wang *et al.*[75] used MIL-125(Ti) as a solid-state electrolyte matrix, and used ZnMOF-808 with microporous structures featuring nano-wetting interfaces that are restricting and guiding uniform zinc deposition; the Ti–O bonds resisted electrolyte corrosion, and the Ti^{3+}/Ti^{4+} redox couple promoted Zn^{2+} transport (Fig. 6a). The resulting electrolyte had an ionic conductivity of 0.26 mS cm^{-1}, enabling the Zn symmetric battery to cycle for 1500 h.

The size and surface state of metal clusters directly affect the number of exposed zincophilic sites. For example, $Zr_6O_4(OH)_4$ clusters in UiO-66 have 12 coordination sites, 6 of which are occupied by –OH groups—these –OH groups act as zincophilic sites to anchor Zn^{2+}.[52] For cluster defect engineering, creating defects in metal clusters can increase the number of exposed active sites. We have mentioned that Lei *et al.*[52] prepared UiO-67-2D nanosheets with $Zr_6O_4(OH)_4$ cluster defects; the defect density increased the concentration of Zr–OH sites by 40%, enhancing the Zn^{2+} adsorption capacity. The UiO-67-2D@Zn anode had a lower nucleation overpotential (22.1 mV) than defect-free UiO-67 (35.7 mV) and cycled for 800 h without short-circuiting. For bimetallic clusters, introducing a second metal into clusters can synergistically improve zinc affinity and conductivity. For example, Zn–Zr bimetallic clusters in UiO-66 increased the number of Zn^{2+} adsorption sites by 30% compared with monometallic Zr clusters, while maintaining high stability (Fig. 6b).[76] The bimetallic MOF-coated Zn anode cycled for 2000 h at 1 mA cm^{-2}, with a CE of 99.8%.

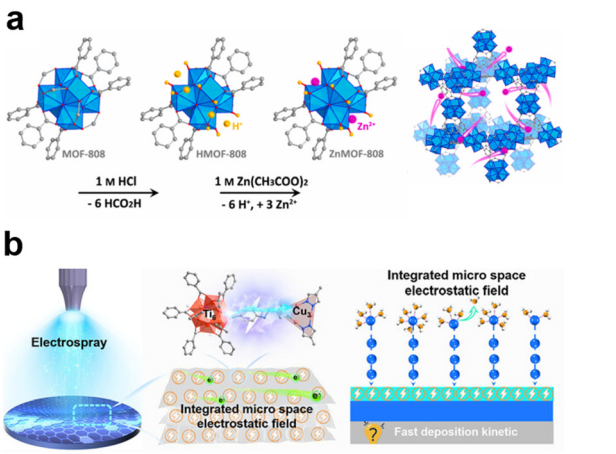

Fig. 6 (a) Scheme for the post-synthetic modification chemistry and crystal structure of ZnMOF-808. Blue polyhedra represent Zr–O clusters and Zn^{2+} ions are highlighted by pink balls. Reproduced with permission from ref. 75 Copyright 2019, Elsevier. (b) Schematic of electrospraying applied for scalable fabrication of the hetero-metallic cluster MCOF–Ti_6Cu_3 nanosheet-coating with integrated micro-space electrostatic field for anode protection. Reproduced with permission from ref. 76 Copyright 2023, Wiley-VCH.

3.2. Adjustments to the intrinsic physical structures of COFs

Covalent organic frameworks exhibit exceptional tunability in their intrinsic physical structures, including pore size, membrane thickness, dimensionality, and microscopic morphology. These structural features directly govern ion transport kinetics, electric field distribution, and interfacial stability at the metal anode/cathode–electrolyte interface, thereby enabling precise regulation of Zn^{2+} deposition behavior and effective inhibition of dendrite growth. Furthermore, COF materials, with their covalent structure, possess stronger chemical bonds; using strategies such as incorporating redox-active groups and optimizing pore structures to enhance the utilization of active sites holds promise for achieving better-performing COF cathode materials. This section systematically summarizes the design principles and performance enhancements of COFs through intrinsic physical structure adjustments, supported by representative cases from the referenced literature. Although many imine-linked COFs are reported that can hydrolyze in water, based on the literature, some linkages in COFs demonstrate superior aqueous stability for AZIBs, primarily due to their enhanced chemical inertness. These functional COFs with linkages can achieve stable operation in aqueous electrolytes through hydrolysis resistance.

3.2.1. Pore size regulation. The pore size of COFs is a core parameter that determines the efficiency of Zn^{2+} transport and the ability to screen interfering species. By tailoring pore dimensions through monomer selection and topological design, COFs can achieve effects of ion sieving and flux homogenization, addressing the root cause of uneven deposition-induced dendrite formation for anodes and inhibiting large volume expansion and structural collapse during the Zn^{2+} insertion process for cathodes.

For Zn metal anodes, An and colleagues[77] synthesized covalent organic framework protective coatings (TpPa–COFs) of the zinc anode using 1,3,5-tricarbonylresorcinol (Tp) and *p*-phenylenediamine (Pa) as monomers with a well-defined one-dimensional pore structure (~1.3 nm) by employing liquid–liquid interfacial polymerization. This pore size ensures high throughput of Zn^{2+} ions while preventing the passage of other anions. It was found by XRD tests that the crystallinity of the COF material gradually decreases with the increase of

thickness. In addition, the abundant zincophilic groups in the COF film can even out the Zn^{2+} flux and make it uniformly deposited, thus effectively inhibiting the generation of dendrites. Meanwhile, the excellent hydrophobicity of the carbonyl-rich COF film can accelerate the Zn^{2+} desolvation process and significantly reduce the corrosion reaction. In electrochemical tests, the COF@Zn anode was stably cycled for 300 h at 1 mA cm^{-2} (Fig. 7a).

For Zn metal cathodes, Banerjee and colleagues first reported that a hydroquinone-linked β-ketoenamine COF (referred to as HqTp COF) could be used as the cathode of zinc-ion batteries (Fig. 7b).[78] During the electrochemical REDOX process, the abundant C═O and N–H functional groups in the structure can effectively coordinate with Zn^{2+} in a reversible manner. In addition, the interlayer spacing and unique pore size (1.5 nm) of HQTT–COF can accommodate a large amount of Zn^{2+} between the two-dimensional layers and promote the migration of Zn^{2+}, thereby enabling zinc-ion batteries to exhibit excellent electrochemical performance. It is worth noting that at a current density of 125 mA g^{-1}, its discharge capacity is as high as 276.0 mAh g^{-1}. At a current density of 3750 mA g^{-1}, the discharge capacity is 85.0 mAh g^{-1}. After 1000 cycles, it can still maintain 95% of its initial capacity, with a coulombic efficiency as high as 98% and no attenuation at all. This work indicates that designing appropriate functional groups is a key factor in enhancing the Zn^{2+} storage capacity of COF cathodes. Based on previous research, Liu and his team introduced Tp–PTO–COF as the cathode, which has multiple carbonyl active sites, including adjacent carbonyl and β-ketone carbonyl, to further enhance the electrochemical performance of zinc-ion batteries (Fig. 7c).[79] The author, through rigorous theoretical calculations and experimental analyses, clarifies that Tp–PTO–COF stores charge through the coordination of zinc ions with oxygen atoms.

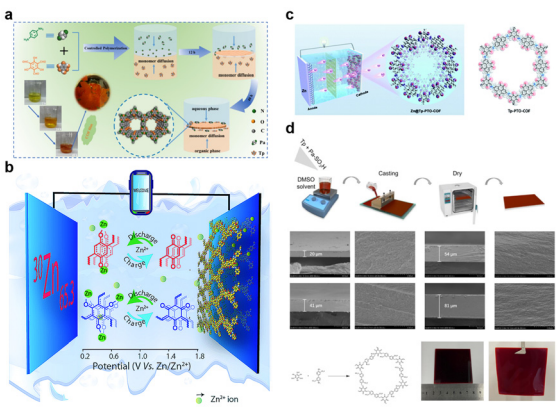

Fig. 7 (a) Schematic illustration of the general design of TpPa–COF materials. Reproduced with permission from ref. 77 Copyright 2025, Elsevier. (b) Schematic of a hydroquinone stitched β-ketoenamine COF acting as an efficient organic cathode in an AZIB. Reproduced with permission from ref. 78 Copyright 2019, Elsevier. (c) Tp–PTO–COF with multiple carbonyl active sites is synthesized and successfully introduced in AZIBs. Reproduced with permission from ref. 79 Copyright 2022, Elsevier. (d) Schematic of formation of TpPa–SO_3H COF films. Reproduced with permission from ref. 80 Copyright 2025, Elsevier.

3.2.2. Membrane thickness optimization. The thickness of COF membranes directly affects two contradictory requirements: mechanical robustness to resist dendrite piercing and ion transport efficiency to avoid excessive polarization. Excessive thickness increases ion diffusion pathways and interfacial impedance, while insufficient thickness leads to structural and dendrite penetration. Literature studies have identified a "critical thickness window" for different metal anodes, balancing these trade-offs.

Park *et al.*[53] reported a 70 nm-thick DIP-D COF membrane: this thickness achieved a Young's modulus of 0.1–0.2 GPa, flexible enough to accommodate volume changes during Zn plating/stripping while maintaining puncture resistance. Thinner membranes (<50 nm) led to dendrite penetration through pores, while thicker membranes (>100 nm) caused mechanical brittleness and impedance increase (R_{ct} > 80 Ω). The DIP-D@Zn||δ-MnO_2 full cell retained 88.5% capacity after 300 cycles at 2 A g^{-1}, compared with 58.7% for bare Zn.

Li *et al.*[80] conducted experiments at 50 °C using the low-temperature crystallization method (LTCM), resulting in the formation of densely packed TpPa–SO_3H COF films on a flat substrate (Fig. 7d). By using a larger substrate, a larger and more complete TpPa–SO_3H COF film was obtained. The SEM image of this film shows a large-scale, continuous and smooth structure. Cross-sectional analysis confirmed a dense morphology with a thickness of approximately 20 μm. The micro-computed tomography images further confirmed the dense structure of the film. By adjusting the casting thickness during the synthesis process, films of different thicknesses ranging from 20 to 80 μm can be obtained. This method can be extended to the synthesis of other COFs based on Schiff base reactions. Using Tp and 4,4′-diaminobiphenyl-3,3′-disulfonic acid (BD–SO_3H) as precursors, completely uniform membranes were successfully obtained, demonstrating the multifunctionality of this method.

3.2.3. Dimensionality design. COFs exhibit distinct structural advantages in 2D and 3D configurations, which are tailored to different challenges of Zn anodes: 2D is suitable for ordered ion channels, 3D is suitable for volume expansion buffering.

2D COFs featuring parallel layered structures with interlayer channels are typically 3–4 Å and have in-plane ordered pores, enabling fast ion transport through "layer-parallel diffusion" and uniform active site distribution. For anodes, Yang *et al.*[81] employ the phase-transfer polymerization (PTP) method to prepare 2D iCOF nanosheets, which are deposited on the surface of a Zn metal anode. The formed iCOF SEI tightly adheres to the Zn anode and can suppress the chemical corrosion. Besides, the porous structure and abundant zincophilic sites of iCOF SEI produce a uniform Zn^{2+} flux and fast desolvation that result in a stable and homogeneous Zn^{2+} deposition. Attributed to the structural advantages of iCOF-ED layer, a remarkable performance can be achieved with affordable Zn plating/stripping behavior over 1000 h at 1 mA cm^{-2} in sym-

metric cells and long-term cycling stability of 1130 cycles at 2 A g^{-1} in half cells (Fig. 8a). The anode maintained a CE of 99% after 1000 cycles, with no dendrite formation observed.

3D COFs possess interconnected pore networks and spatial confinement effects, which address the critical issue of volume expansion of about 100% for Zn during cycling. Wu *et al.*[49] constructed a 3D-COOH–COF with a hierarchical pore structure: the 3D skeleton buffered volume changes by accommodating deposited metal, and the interconnected 1.3 nm pores increased Zn^{2+} active site exposure. The 3D-COOH–COF@Zn symmetric cell achieved a record cycling life of 2000 h, far exceeding the 600 h of 2D TpPa–COF@Zn. Similarly, Guo *et al.*[82] prepared a 3D MXene@COF composite: the MXene nanosheets formed a conductive skeleton, while the 3D COF pores (1.6–1.8 nm) regulated Zn^{2+} flux (Fig. 8b). The composite anode exhibited a low polarization voltage of 24 mV at 1 mA cm^{-2}, with stable cycling for 1600 h. These results confirm that 3D COFs are more suitable for high-areal-capacity scenarios >5 mAh cm^{-2}, while 2D COFs excel in low-impedance, high-rate applications.

3.2.4. Microscopic morphology engineering. The microscopic morphology of COFs directly modulates the anode surface's current density distribution and electrolyte wettability. By designing hierarchical morphologies, COFs can reduce local current density hotspots and enhance interfacial adhesion, further suppressing dendrite growth.

Flower-like morphology: Hu *et al.*[63] synthesized a flower-like COF–H with petal-like nanosheets: the hierarchical structure increased the specific surface area to 1860 m^2 g^{-1}, reducing the local current density from 5 to 1.2 mA cm^{-2}. The AA-stacking mode of COF–H enhanced the chemical stability, and the alkynyl-rich pores promoted Zn^{2+} uniform deposition. The COF–H@Zn symmetric cell cycled stably for 900 h at 3 mA cm^{-2}, with no corrosion observed.

Honeycomb morphology: He *et al.*[83] developed a honeycomb-like G–COF with periodic 2.5 nm nanochannels: the hexagonal pores provided zincophilic sites such as $-OCH_3$ or $-C{\equiv}N$, reducing the Zn^{2+} nucleation overpotential from 62 to 33 mV (Fig. 8c). The negative potential (−24.5 mV) of G–COF repelled SO_4^{2-}, inhibiting the formation of $Zn_4SO_4(OH)_6{\cdot}4H_2O$ byproducts. The G–COF@Zn symmetric cell maintained stable cycling for 1650 h at 3 mA cm^{-2}.

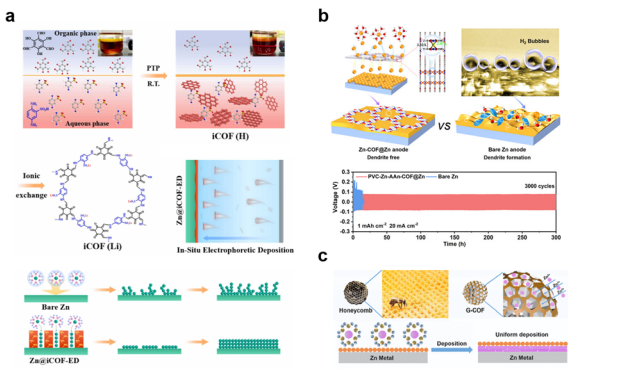

Fig. 8 (a) Scheme of the 2D iCOF nanosheets. Reproduced with permission from ref. 81 Copyright 2023, Elsevier. (b) Structures and properties of 3D MXene@COF composite. Reproduced with permission from ref. 82 Copyright 2022, Wiley-VCH. (c) Scheme of honeycomb-like G–COF. Reproduced with permission from ref. 83 Copyright 2025, American Chemical Society.

4. Battery component modification by MOFs and COFs

The intrinsic structural tunability of MOFs and COFs lays a solid foundation for their application in battery component modification.[84] In practical battery systems, performance bottlenecks extend beyond anode dendrite growth to involve multiple components: cathodes suffer from active material dissolution and low ion diffusion efficiency, separators lack ion selectivity and anti-dendrite penetration capability, and electrolytes face poor interfacial compatibility and side reaction promotion. MOFs and COFs, with their multi-functional synergistic advantages, integrating ion regulation, a physical barrier, and active site catalysis, can target the pain points of different components, constructing a component-level collaborative optimization system to comprehensively enhance battery performance. MOFs, relying on the flexible coordination of metal nodes and organic ligands, exhibit diverse adjustment strategies in component modification. Their tunable pore structures match hydrated Zn^{2+} diameters for precise ion sieving, while metal nodes with strong coordination bonds ensure structural stability in aqueous electrolytes—key to addressing anode dendrite growth, cathode material leaching, and separator mechanical weakness.[24] COFs, built *via* covalent bonding of organic building units, have unique advantages in component modification. Their ultra-stable covalent skeletons resist electrolyte erosion, making them suitable for long-cycle modification of separators and electrolytes. Functional groups on COFs enable zincophilic nucleation guidance, hydrophobic electrolyte isolation, and local pH regulation—effectively suppressing anode HER and dendrite growth. Additionally, COFs' ordered nanochannels enhance ion selectivity when modifying separators, while their high specific surface area boosts cathode material loading and utilization. The following will first elaborate on the modification mechanisms and applications of MOFs in each battery component, then systematically discuss COFs' role in component optimization, forming a comprehensive analysis of the two framework materials in advancing battery performance.

4.1. Battery component modification by MOFs

Metal–organic frameworks, with their designable porous structures, tunable surface functional groups, and diverse metal node properties, exhibit remarkable versatility in modifying key battery components. By leveraging their synergistic effects, MOFs can address critical issues of different components in AZIBs, such as dendrite growth, active material dissolution, low ion conductivity, and interfacial instability. This section

systematically summarizes the application of MOFs in modifying battery components, combining cutting-edge research progress from the provided literature.

4.1.1. MOFs as anode-protective coatings. The Zn metal anode, a core component of AZIBs, faces critical challenges including dendrite growth, HER and unstable SEI. MOFs act as artificial protective coatings on the Zn anode surface, integrating the multi-functions of ion flux regulation, physical dendrite blocking and interfacial stabilization to extend battery cycle lifespan, with their design for AZIBs focusing on three core strategies targeting dendrite growth, HER, and Zn corrosion.

The channel sizes of MOFs act as the key control factor to balance the zinc ion flux and Zn^{2+} desolvation behavior within the channels and between the intergranular spaces. Zhang *et al.*[85] propose three coating layers made by MOFs; among these layers, the MOF-5 W layer with confined spaces and channels is capable of promoting the spontaneous desolvation process (Fig. 9a). The activated surface sites on MOF-5 W endow the intergranular channels with accelerated ion transportation and spontaneous Zn^{2+} desolvation. The two kinds of migration path are well-matched, as the MOF-5 W@Zn anode shows Zn stripping/plating over 5000 cycles at 40 mA cm^{-2}, as well as cycling stability of 1050 h with a high areal capacity of 10 mAh cm^{-2}.

Liu and his colleagues[86] presented a new perspective on the strategy of adding zincophilic sites to MOFs as a protective layer. They have developed a copper-based MOF as a zinc anode protective layer *via* a simple solution method for AZIBs (Fig. 9b). Synchrotron XRD and XAS data show that substituting Cu and Co atoms for some Zn sites into ZIF-L does not alter the framework structure. More importantly, zincophilic sites guide the uniform deposition of Zn^{2+} and suppress dendrite production due to their large nucleation sites. The symmetric cell can keep cycling for 800 hours even at a large current density of 5 mA cm^{-2} with an areal capacity of 1.0 mAh cm^{-2}. Moreover, the full cell with an MnO_2 cathode exhibits a stable cycling life with 189 mAh g^{-1} after 700 cycles at 1.0 A g^{-1}.

Recently, the hot-press solution (HTS) is proposed as a versatile and cost-effective strategy for *in situ* modification of separators with various MOF materials to address dendrite-related issues in Zn anodes. Wang *et al.*[87] developed an HTS that was modified by *in situ* MOF crystals on the fiber surface without the obstruction of the original pore structure (Fig. 9c). On the Zn negative electrode, particularly the region obscured by the separator, dendrites and dead zinc are effectively restrained by the HTS. Furthermore, the mechanisms of the dynamic concentration–regulation process were characterized by involving the guidance of homogeneous nucleation at high concentrations and the promotion of two-dimensional crystal growth at low concentrations, attributed to the interfacial high concentration and the slow diffusion kinetic of the HTS. Based on the aforementioned characteristics, HTS enables a high stability of the anode accompanied by a long cycling life of 3000 h at 2 mA cm^{-2}/2 mAh cm^{-2} and 4900 h at 1 mA cm^{-2}/1 mAh cm^{-2}. For the Zn||I_2 full cell, the HTS allowed for a long cell life of 15 000 cycles at 1 A g^{-1}. A 120 mAh Zn||I_2 pouch cell could also realize 80 cycles with a 800 mAh high capacity.

4.1.2. MOFs as cathode carriers/catalysts. Cathodes in Zn batteries often suffer from low active material utilization, poor conductivity, and dissolution. Several types of cathode material for AZIBs have been studied, such as manganese-based cathodes,[88–90] vanadium-based cathodes[91,92] and quinone.[93,94] However, these cathodes face several challenges such as rapid capacity fading and serious toxicity. MOFs act as cathode carriers or catalysts to address these issues by virtue of their high specific surface area, porous structure, and metal node catalytic activity—their crystalline frameworks not only provide stable support for active materials but also tune redox behavior and ion diffusion *via* adjustable metal nodes and organic linkers, aligning with the "structure–performance" correlation of MOF materials.[95]

In AZIBs, MOFs improve the conductivity and stability of transition metal oxide cathodes while enabling direct application as active cathodes *via* intrinsic redox activity. When used as carriers, MOFs' confined pores inhibit active material dissolution and enhance electron transfer. Mondal *et al.*[96] applied V-based MIL-100(V) as a cathode carrier (Fig. 10a); its 3D zeolite-like structure with dual mesoporous cages (2–5 nm) facilitated Zn^{2+} transport, and V^{4+}/V^{5+} redox couples in metal nodes, and synergistically enhanced capacity, achieving 362 mAh g^{-1} at 0.2 A g^{-1}. MOFs can also serve as direct cathode active materials by leveraging redox-active metal nodes and organic linkers. Nam *et al.*[97] employed $Cu_3(HHTP)_2$ (HHTP = 2,3,6,7,10,11-hexahydroxytriphenylene) as a cathode (Fig. 10b), which features stacked π-conjugated 2D layers and 1D channels of ~1.2 nm. Both Cu^{2+} nodes and quinoid groups in HHTP participate in Zn^{2+} storage, contributing to a high reversible capacity of 228 mAh g^{-1} at 50 mA g^{-1}.

For vanadium-based cathodes, Ru *et al.*[98] synthesized V-MIL-47 with 1D layered channels and V^{4+}/V^{5+} redox-active

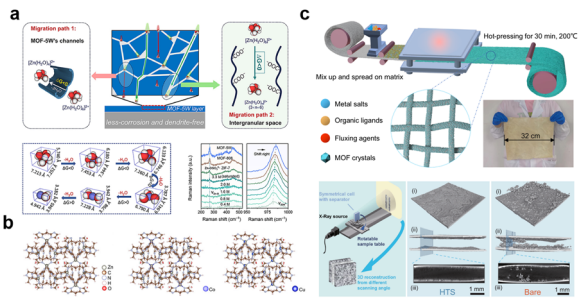

Fig. 9 (a) Scheme of the channel sizes of MOFs as the key control factor to balance the zinc ion flux and Zn^{2+} desolvation behaviour. Reproduced with permission from ref. 85 Copyright 2024, Elsevier. (b) Crystal Structures of ZIF-L, Cu and Co based ZIF. Reproduced with permission from ref. 86 Copyright 2025, Wiley-VCH. (c) Scheme of a hot-press solution modified by *in situ* MOF crystals on the fiber surface without the obstruction of the original pore structure. Reproduced under terms of the CC-BY license.[87] Copyright 2025, Springer Nature.

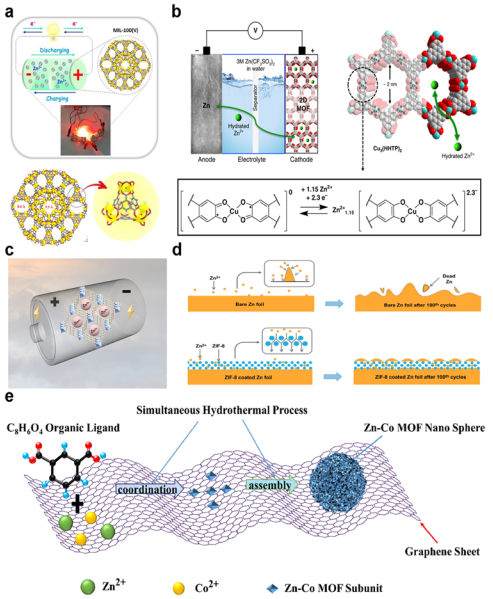

Fig. 10 (a) Scheme structure of MOF-based AZIBs constructed with porous MIL-100(V). Reproduced with permission from ref. 96 Copyright 2023, Elsevier. (b) Structures and properties of a Zn-2D MOF cell with $Cu_3(HHTP)_2$ cathode. Reproduced under the terms of the CC-BY license.[97] Copyright 2019, Springer Nature. (c) Scheme illustration of a V-MOF//Zn battery. Reproduced with permission from ref. 98 Copyright 2021, Elsevier. (d) Schematic illustration for morphology change of the bare Zn foil and ZIF-8@Zn electrodes during repeated Zn stripping/plating processes. Reproduced with permission from ref. 99 Copyright 2020, Springer Nature. (e) Schematic assembly of a Zn–Co MOF nanosphere/rGO by a hydrothermal process. Reproduced with permission from ref. 100 Copyright 2023, Elsevier.

nodes (Fig. 10c). Its pore size is about 8 Å and the high conductivity of 243 mS cm^{-1} for MIL-47 powder promoted rapid Zn^{2+} intercalation, delivering 332 mAh g^{-1} at 100 mA g^{-1} and maintaining 85% capacity after 300 cycles. Additionally, MOF modification *via* ligand functionalization or metal node doping further optimizes cathode performance. As we have illustrated, MOF-808-grafted EDTA[50,55] uses EDTA's chelating sites to accelerate Zn^{2+} diffusion, and Zr^{4+} nodes stabilize the cathode–electrolyte interface; the MOF-E/MnO_2 cathode exhibited a rate capability of 150 mAh g^{-1} at 5 A g^{-1}, 2.5 times higher than pure MnO_2. Pu *et al.*[99] applied Mn(BTC) (BTC = 1,3,5-benzenetricarboxylic acid) as a cathode, where Mn^{2+}/Mn^{3+}/Mn^{4+} redox reactions drive Zn^{2+} storage; the 3D framework of Mn(BTC) inhibits Mn dissolution by confining active sites (Fig. 10d), its electrical conductivity is 2.3 mS cm^{-1} when composited with PEO–CLP polymer and conductivity ensures efficient electron transfer, achieving 138 mAh g^{-1} at 100 mA g^{-1}.

Wu *et al.*[100] developed a bimetallic constructed MOF, Co NS/rGO, with the aim of enhancing the structural stability and synergy of the individual metals used for energy storage and conversion (Fig. 10e). Zn–Co NS/rGO is used to fabricate an asymmetric supercapacitor that matches a 3D rGO aerogel anode. The fabricated devices exhibit excellent performance, including a broadened operating potential window of 1.5 V, an energy density of 43.04 W h kg^{-1} at a power density of 900 W kg^{-1}, and an energy density of 14.166 W h kg^{-1} at a power density of 75 000 W kg^{-1}.

4.1.3. MOF-modified separators. The separator, located between the Zn metal anode and cathode, is an essential component of AZIBs. It contains the necessary electrolyte to form ion transport channels and separates the two electrodes to ensure the battery operates normally; separators play a critical role in preventing electrode short-circuiting and regulating ion transport.[24] MOFs modify separators, aiming to enhance ion selectivity, mechanical strength, and anti-dendrite penetration ability, addressing the "ion flux imbalance" and "dendrite piercing" issues of traditional separators.

Ion-selective separators are a relatively common type of separator among MOF-modified separators. MOFs with tailored pores and charged functional groups form ion-sieving layers on separators, allowing Zn^{2+} to pass while blocking anions or soluble intermediates. Mohamed *et al.*[101] investigated the performance and endurance of AZIBs that use MOFs, specifically UiO-66 and UiO-67, to change microfiber glass separators (Fig. 11a). The results showed that symmetrical cells with MOF-modified separators performed exceptionally well, sustaining a steady voltage for more than 400 h at a high current density of 5 mA cm^{-2}. This improvement is due to the improved consistency of zinc ion flux during the stripping and plating operations. Furthermore, MOF-based Zn/MnO_2 cells showed reduced voltage polarization and maintained a high specific capacity after 1000 cycles at 1 A g^{-1}. Maeboonruan *et al.*[102] focused on utilizing MOF-808 and ZIF-8 to modify glass microfiber separators (Fig. 11b). The results demonstrated that the symmetrical cell using MOF-modified separators exhibited high performance, maintaining a stable voltage over 1000 h, attributed to the enhanced uniformity of Zn ion flux during striping/plating processes. Additionally, at the current density of 1.0 A g^{-1}, zinc-ion capacitors with MOF-modified separators exhibited higher specific capacities compared with those using the pristine separators and prolonged the cycle life over 20 000 cycles with a capacity retention of 63.89%. Importantly, the MOF-modified separators can also inhibit non-uniform dendritic zinc growth on a zinc anode surface, according to the scanning electron micrographs.

Mechanical reinforced separators are another important sort of MOF-modified separators. MOFs with high mechanical strength such as Zr-based or Ti-based improve the anti-penetration ability of separators. Liu *et al.*[103] used HKUST-1 ($Cu_3(BTC)_2$) to modify the PE separator; the Cu^{2+} nodes provided zincophilic sites to regulate Zn^{2+} deposition, and the 14 Å truncated octahedral pores buffered volume expansion (Fig. 11c). The HKUST-1/PE separator maintained structural integrity after 500 cycles, with no dendrite penetration observed *via* SEM. Zhao *et al.*[104] examines how the morphology of HKUST-1-based MOFs affects the mechanical strength of the separators and finally affects the performance of AZIBs (Fig. 11d). Three HKUST-1 morphologies were synthesized, namely orthorhombic octahedral, semi-fused, and fully-fused, and were integrated with cellulose nanofibers to create compo-

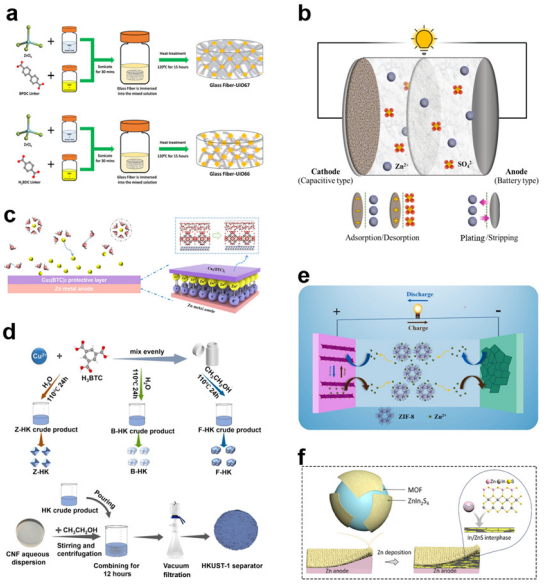

Fig. 11 (a) Scheme synthesis of UiO-67–GF and UiO-67–GF. Reproduced with permission from ref. 101 Copyright 2025, Elsevier. (b) Schematic diagram of zinc-ion hybrid capacitors consisting of porous carbon cathodes and zinc anodes. Reproduced with permission from ref. 102 Copyright 2024, Elsevier. (c) Schematic diagram of the modification of a polyethylene (PE) separator by HKUST-1 ($Cu_3(BTC)_2$). Reproduced with permission from ref. 103 Copyright 2024, Elsevier. (d) Flowchart for the preparation of different morphologies of HKUST-1 and flow chart for the preparation of HKUST-1@CNF battery separators with different morphologies. Reproduced with permission from ref. 104 Copyright 2025, Elsevier. (e) Scheme of ZIF-8 used as an electrolyte additive for AZIBs. Reproduced with permission from ref. 105 Copyright 2023, Elsevier. (f) Scheme illustration of the structure and working mechanism of the M@Z quasi-solid electrolyte. Reproduced with permission from ref. 106 Copyright 2025, Wiley-VCH.

site separators. The fully-fused HKUST-1 (F-HK) separator demonstrated superior performance due to its amorphous network structure, which enhanced mechanical strength, promoted uniform zinc ion deposition, and suppressed dendrite growth. In Zn//Cu half cells, the F-HK separator exhibited a low nucleation overpotential of 47 mV and an average coulombic efficiency of 99.98% over 500 cycles. In Zn//MnO_2 full cells, it retained over 80% capacity after 400 cycles at 1 A g^{-1} with a high CE of almost 100%. Additionally, the F-HK separator showed significantly enhanced mechanical strength compared with pristine cellulose separators. The findings underscore the pivotal role of morphology in enhancing separator performance for AZIBs.

4.1.4. MOFs as electrolyte additives/solid electrolyte matrices. Electrolytes directly affect ion transport and interfacial stability. MOFs act as electrolyte additives or solid-state electrolyte (SSE) matrices to improve ionic conductivity, suppress side reactions, and enhance safety—aligning with the interface stabilization mechanism of MOFs in dendrite inhibition.

In liquid electrolyte additives, few reports currently use MOFs as the liquid electrolyte additive for AZIBs. In this scenario, MOFs as additives adsorb free ions or regulate solvation structures to homogenize ion flux. Gong *et al.*[105] added ZIF-8 nanoparticles (0.5 wt%) to 2 M $ZnSO_4$ electrolyte. ZIF-8 is a common molecular sieve imidazole framework, with high hydrophobicity, chemical and thermal stability (Fig. 11e). Recently, ZIF-8 has attracted a lot of attention in the field of AZIBs. The ZIF-8 adsorbed Zn^{2+} *via* Zn–N coordination bonds, reducing local ion concentration fluctuations and the nucleation overpotential from 62 mV to 28 mV. The ZIF-8-added electrolyte enabled the Zn||MnO_2 battery to cycle for 600 cycles at 1 A g^{-1}, with a capacity retention of 88%—compared with 58% for pure electrolyte.

In SSE matrices, MOFs with high porosity and thermal stability serve as SSE matrices to accommodate ionic liquids or salt solutions, addressing the low conductivity and poor safety of traditional SSEs. Wang *et al.*[75] infiltrated $Zn(TFSI)_2$ into MOF-808 pores (pore volume 1.2 cm^3 g^{-1}) to form a single-ion SSE; the Zr^{4+} nodes coordinated with $TFSI^-$ to promote Zn^{2+} transport, achieving an ionic conductivity of 0.26 mS cm^{-1} at 25 °C. The MOF-808-based SSE suppressed Zn dendrite growth and the HER, enabling the Zn||Zn symmetric cell to cycle for 1500 h. Li and colleagues[106] have developed a quasi-solid electrolyte that is based on an MOF@$ZnIn_2S_4$ composite (Fig. 11f). This novel electrolyte features high room-temperature conductivity, reaching 0.99 mS cm^{-1}, along with an enhanced Zn^{2+} transference number of 0.54. The microporous structure of the MOF component plays a key role in enabling uniform Zn deposition and effectively inhibiting the growth of dendrites. In the meantime, the $ZnIn_2S_4$ nanosheets that encapsulate the MOF particles facilitate the formation of a favorable interphase containing In and ZnS on Zn anodes during cycling. This interphase helps reduce side reactions and speeds up the reaction kinetics at the anode. Benefiting from these effects, Zn symmetric cells using this electrolyte can maintain stable Zn plating and stripping for over 3130 h with a low overpotential, while also withstanding a high critical current density of 10 mA cm^{-2}. Additionally, vanadium-based full cells assembled with the M@Z electrolyte demonstrate excellent cycling stability, showing nearly no capacity decay after 1000 cycles at a current density of 1.0 A g^{-1}.

4.2. Battery component modification by COFs

Covalent organic frameworks, featuring designable crystalline porous structures, tunable surface functional groups, and exceptional chemical stability, exhibit versatile modification effects on key components of AZIBs. Compared with MOFs, COFs have a wider range of applications in low-temperature environments due to their covalent bonds, so COFs can address critical issues of different battery components in special environments, thereby comprehensively enhancing battery performance. This section systematically summarizes the application of COFs in modifying battery components, integrating cutting-edge research progress from the provided literature.

4.2.1. COFs as anode protective layers. COFs serve as artificial protective layers on anode surfaces, integrating multiple

functions to construct a stable anode–electrolyte interphase (AEI), which is the core to extending battery cycle life. COF layers focus on suppressing Zn dendrite growth, HER, and corrosion—issues exacerbated by the thermodynamic instability of Zn in aqueous systems.

Coating COFs with $-SO_3H$, –COOH or nitrogen-containing zincphilic functional groups on the anode of ABIZs can reduce the nucleation overpotential of Zn^{2+} and guide its horizontal deposition along the low-energy (002) crystal plane. These zincphilic functional groups can induce uniform nucleation. Zhao *et al.*[51] synthesized a $-SO_3H$-functionalized TpPa–SO_3H COF as an anode protective layer, and the sulfonic oxygen atoms formed strong coordination bonds with the Zn^{2+}, reducing the nucleation overpotential from 95 mV for bare Zn to 39 mV. Fluorinated or alkynyl-rich COFs reduce water molecule penetration, suppressing the HER and the formation of by-products such as $Zn_4SO_4(OH)_6{\cdot}xH_2O$. Li *et al.*[107] developed an imine-based COF (COF–S–F) containing $-SO_3H$ and –F groups as the SEI layer for ZMA (Fig. 12a). The highly electronegative $-SO_3H$ and hydrophobic –F groups stabilize the active H_2O molecules in the electrolyte, facilitating the desolvation process of hydrated Zn^{2+}. As a result, the corrosion current density of the Zn@COF–S–F symmetric cell (0.942 mA cm^{-2}) is significantly lower than that of the bare Zn symmetric cell (3.405 mA cm^{-2}). Additionally, due to electrostatic repulsion, sulfate ions migrating from the electrolyte to the ZMA are repelled. The large amounts of H generated by the ionization of $-SO_3H$ neutralize OH^- in the ionic H_2O, which helps suppress the formation of parasitic products such as $ZnSO_4{\cdot}3Zn(OH)_2{\cdot}5H_2O$. Hu *et al.*[63] prepared a flower-like COF–H with alkynyl units (water contact angle 141°); its hydrophobic pores blocked H_2O access to Zn, reducing the HER rate to 0.03 mL h^{-1}, which is about 1/20 that of bare Zn. The COF–H@Zn symmetric cell cycled stably for 900 h at 3 mA cm^{-2}, with no corrosion products detected by SEM. 3D COFs with interconnected pores accommodate Zn deposition, avoiding protective layer rupture caused by volume changes. Wu *et al.*[49] constructed a 3D-COOH–COF with the pore size of 1.3 nm on Zn metal; the 3D skeleton buffered volume expansion by 80%, and the negatively charged –COOH groups repelled SO_4^{2-} to inhibit side reactions. The 3D-COOH–COF@Zn symmetric cell achieved a record cycling life of 2000 h at 1 mA cm^{-2}, compared with only 112 h for bare Zn.

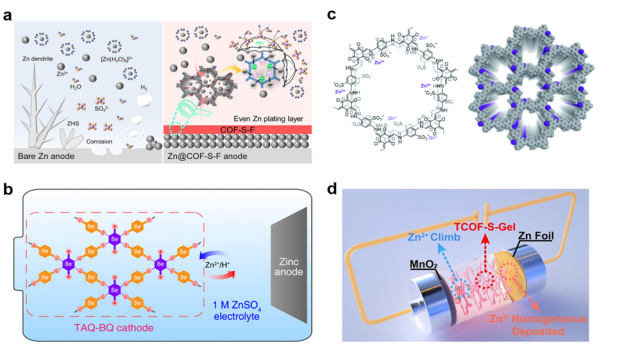

Fig. 12 (a) Schematic illustrations of Zn@COF–S–F with dendrite-free morphology and suppressed side reactions. Reproduced with permission from ref. 107 Copyright 2024, Elsevier. (b) Schematic of a full anti-aromatic microporous COF cathode material of TAQ–BQ designed for aqueous zinc batteries. Reproduced with permission from ref. 108 Copyright 2022, American Chemical Society. (c) Schematic chemical structure of TpPa–$SO_3Zn_{0.5}$. Reproduced with permission from ref. 109 Copyright 2020, Royal Society of Chemistry. (d) Schematic illustrations of the operation perspective diagram of a Zn||MnO_2 full battery based on TCOF-S-Gel quasi-solid electrolyte. Reproduced with permission from ref. 110 Copyright 2023, Elsevier.

4.2.2. COFs as cathode carriers. Cathodes in Zn batteries often suffer from low active material utilization, poor electron conductivity, and dissolution. Consequently, while the merits of MOFs/COFs for anode stabilization can be convincingly demonstrated even with thin films operating at lower potentials and in milder environments, establishing their viability for cathodes presents a significantly greater challenge, which must maintain stability under high mass loading and high-rate conditions. Similar to MOF materials, the zinc storage mechanism in COFs is not solely determined by their pore structure. The coordination effects of functional groups and the type of electrolyte used also play a role in shaping their zinc storage mechanism during operation. COFs act as cathode carriers or electrocatalysts to address these issues, leveraging their high specific surface area of about 1000–3000 m^2 g^{-1}, tunable pores, and functional groups' catalytic activity. In AZIBs, COFs enhance the conductivity and stability of transition metal oxide cathodes by suppressing active material dissolution and accelerating Zn^{2+} diffusion.

As cathode carriers, COFs can not only increase the REDOX potential but also provide energy storage sites. Lin *et al.*[108] synthesized TAQ-BQ COF material through the condensation reaction between tetraamino-*p*-benzoquinone (TABQ) and benzoquinone (BQ) (Fig. 12b). In aqueous zinc batteries, the TAQ–BQ cathode can provide a high reversible capacity of 208 mAh g^{-1} at a current density of 0.1 A g^{-1}. It can still maintain a capacity of 136 mAh g^{-1} at a current density of 2 A g^{-1}. A stable cycle can still be achieved after cycling 1000 cycles at a current density of 1 A g^{-1}. Mechanism studies have confirmed that both the C=O and C=N centers exhibit electrochemical activity, and co-deintercalation/intercalation of Zn^{2+} with protons occurs in weakly acidic zinc sulfate electrolyte. This study provides an effective approach to enhance the REDOX potential of COF cathode materials for aqueous zinc batteries and introduce multiple cation storage sites. Ma *et al.*[79] adopted approaches to boost the number of active sites and extend the conjugated plane, with the goal of enhancing the electrochemical performance of cathode materials in AZIBs. They fabricated Tp–PTO–COF through the combination of 2,7-diaminopyrene-4,5,9,10-tetraone (DAPTO)—acting as the active component—and Tp. Tp–PTO–COF is characterized by dual active sites formed by adjacent carbonyl and β-keto-carbonyl groups; these groups act as nucleophilic centers, offering reversible and high-efficiency Zn^{2+} storage sites during charging and discharging processes. Furthermore, its ordered

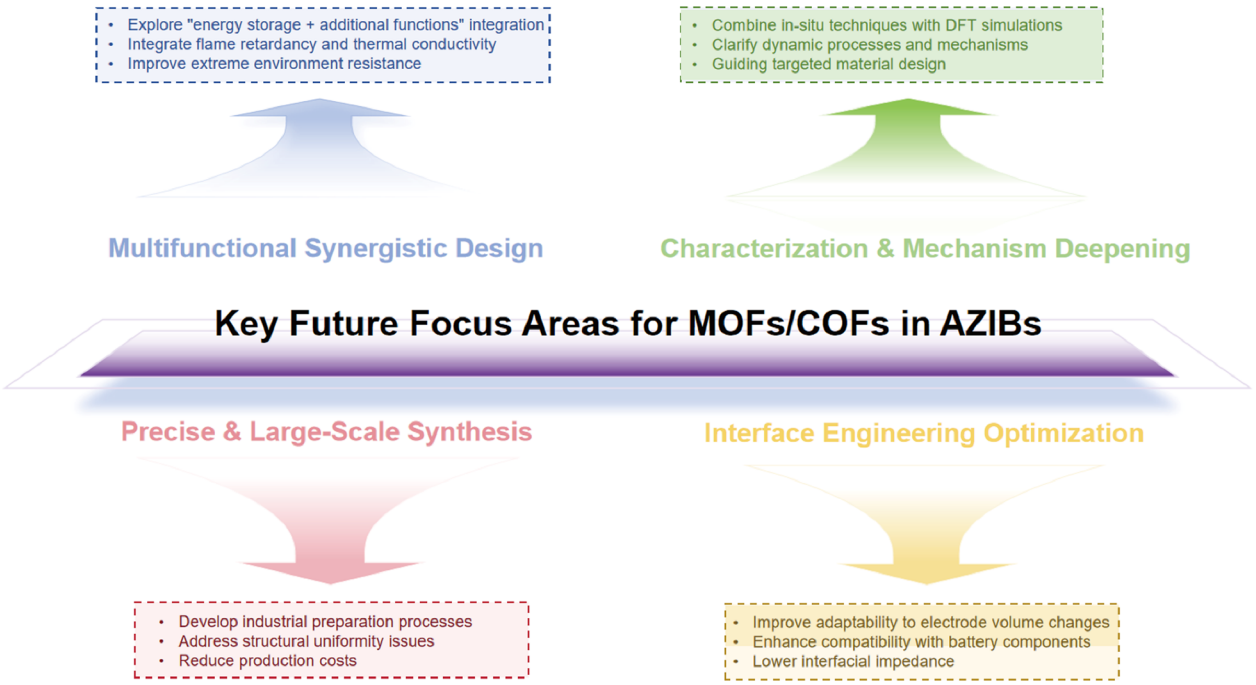

Fig. 13 Schematic illustrations of MOFs/COFs addressing the key challenges of AZIBs in the future.

porous structure and intrinsic chemical stability contribute to fast ion diffusion.

4.2.3. COFs as electrolyte additives/separators. At present, as electrolyte additives or separators for zinc-ion batteries, COF materials are still in the preliminary stage, and they confront a series of challenges.[111] These challenges include inferior ionic conductivity, low stability, restricted capacity to inhibit parasitic reactions, high production expenses, and the difficulty of dissolving water-insoluble COFs that lack hydrophilic groups.[112] Thus, it is crucial to explore innovative framework structures to synthesize COF-based electrolyte additives with improved performance. In addition, the problem of COF consumption during the reaction process also needs to be solved. Consequently, the development of COF-based strategies like quasi-solid-state electrolytes (QASE) or gel polymer electrolytes (GPEs) has great potential for promoting future progress in this field.

COFs are considered highly promising ion-conducting materials due to their ordered porous structure, functionality, and structural stability. COF nanoparticles additives can also adsorb free ions or regulate solvation structures to homogenize ion flux and suppress side reactions, increasing the number of cycles and coulombic efficiency. Park *et al.*[109] introduce a novel category of single-ion conducting electrolytes derived from a zinc sulfonated covalent organic framework: TpPa–$SO_3Zn_{0.5}$ (Fig. 12c). TpPa–$SO_3Zn_{0.5}$ is engineered to display single Zn^{2+} conductive properties through its delocalized sulfonate groups, which are covalently attached to directional pores, while its β-ketoenamine linkages ensure structural stability. Benefiting from these structural and physicochemical characteristics, TpPa–$SO_3Zn_{0.5}$ enhances the redox stability of the zinc metal anode and functions as an ionomeric buffer layer to stabilize the MnO_2 cathode. These improvements at the TpPa–$SO_3Zn_{0.5}$–electrode interfaces, combined with favorable ion transport behaviors, allow aqueous Zn–MnO_2 batteries to achieve long-term cycling performance, thereby validating the feasibility of COF-based electrolytes in AZIBs. Qiu *et al.*[110] reported a sulfonic acid modified COF-based gel electrolyte (TCO-S-gel). As an initiator for acrylamide polymerization, sulfonic acid groups with photoresponsive characteristics are distributed in the channels of TCF-S, initiating the instantaneous *in situ* polymerization of acrylamide and forming a stable gel within the channels (Fig. 12d). The assembled Zn||TCOF-S-Gel||MnO_2 full battery exhibits a high discharge capacity (248 mAh g^{-1} at 1C), excellent rate capability (90 mAh g^{-1} at 10C) and superior cycling performance.

5. Conclusions and perspectives

This review systematically summarizes the cutting-edge progress of MOFs and COFs in addressing the key challenges of AZIBs, and establishes a "structure–performance–material" logical framework centered on these porous framework materials. They are endowed with designable porous structures, tunable surface properties, and high stability. The optimization of MOFs/COFs for AZIBs mainly follows two core pathways: intrinsic physical structure adjustment and battery component modification. For intrinsic structure adjustment, MOFs focus on the optimization of pore size, surface func-

tional groups, and metal nodes, while COFs emphasize the tuning of pore dimensions, membrane thickness, and dimensionality. For battery component modification, MOFs/COFs act as protective coatings for Zn anodes, carriers/catalysts for cathodes, modified layers for separators, and additives/matrices for electrolytes. These applications effectively enhance key battery performances, while clarifying the intrinsic correlation between material design and battery performance, thus providing guidance for the targeted development of framework materials.

Despite the fact that MOFs/COFs have already undergone certain application explorations in AZIBs and demonstrated positive effects in aspects like zinc dendrite inhibition and interface stability optimization, the practical application of these materials still faces numerous challenges. Some research studies of COFs in AZIBs are just at the original stage, and some of the working mechanisms of MOFs/COFs on AZIBs are unclear, so we need to delve into their properties too. Thus, future research should focus on the following key breakthroughs (Fig. 13):

First, precise synthesis and large-scale preparation: addressing issues of poor structural uniformity and high cost in mass production, which are major bottlenecks hindering their industrialization. Traditional solvothermal synthesis often leads to inconsistent pore size distributions and agglomeration of MOF/COF particles, directly affecting their ion transport efficiency and battery performance stability in batch applications. Developing directional synthesis technologies for atomic-level structure control can achieve precise regulation of pore dimensions, functional group positions, and membrane thickness, ensuring that each batch of materials meets the same performance standards. Additionally, exploring low-cost raw materials to significantly reduce production costs is still highly desired. Meanwhile, industrializable processes need to be optimized to improve production efficiency, as current lab-scale synthesis methods cannot meet the large-volume demand of the battery industry.

Second, interface engineering optimization: designing interface transition layers to reduce interface impedance and improve compatibility between frameworks and battery components. The high interfacial impedance between MOFs/COFs and electrodes/electrolytes often arises from poor wettability or weak adhesion. Bare COF membranes typically have an interfacial impedance with Zn electrodes, so developing adaptive framework materials to accommodate electrode volume expansion is critical. Metal anodes can undergo rampant dendrite growth during cycling, and rigid MOF/COF coatings are prone to cracking. However, flexible 2D MOF nanosheets can bend and deform with the anode without structural damage, maintaining continuous protection. 3D COFs, on the other hand, can use their porous skeletons to buffer volume expansion by accommodating deposited Zn, avoiding direct contact between the electrode and electrolyte even when the electrode swells.

Third, multi-functional synergistic design: integrating properties such as flame retardancy, thermal conductivity, and extreme environment resistance to address the multi-dimensional performance requirements of advanced batteries. Introducing different functional groups into MOF ligands can endow the material with flame-retardant, thermal conductivity or other properties. Additionally, exploring the integration of energy storage with other functions can expand the application scenarios of Zn batteries. COFs modified with photothermal materials can absorb sunlight and convert it into heat, which helps melt solid electrolytes in low-temperature environments, enabling batteries to operate normally without external heating devices. This multi-functional integration not only enhances battery safety and adaptability but also adds value to energy storage systems in special fields such as outdoor portable electronics and aerospace.

Fourth, *in situ* characterization and mechanism deepening: in this stage, we are supposed to combine *in situ* techniques with density functional theory (DFT) simulations to track the dynamic structural changes of materials during cycling. Current *ex situ* characterization methods can only capture static states of materials before and after cycling, failing to reveal intermediate processes such as pore blockage by by-products or ligand dissociation under electrochemical stress. Furthermore, we should use DFT simulations to calculate the adsorption energy of Zn^{2+} on MOF/COF active sites and the energy barrier of ion transport, guiding the pre-design of functional groups. By integrating experimental observations and theoretical calculations, the intrinsic mechanisms of dendrite inhibition, side reaction suppression and capacity decline can be fully clarified, avoiding blind material design.

Although the application of MOF/COF materials in AZIBs remains in the exploratory stage, with challenges such as precise large-scale synthesis, interface compatibility optimization, and cost control yet to be fully addressed, their unique advantages—including designable porous structures, tunable surface chemistry, and multi-mechanistic synergy in inhibiting dendrite growth and suppressing side reactions—endow them with immense potential to break through the performance bottlenecks of current AZIB systems. As research progresses in structural regulation, interface engineering, and functional integration, we anticipate that MOF/COF-based strategies will not only accelerate the large-scale application and industrialization of AZIBs but also provide valuable insights for optimizing other emerging rechargeable battery technologies, thereby contributing to the advancement of high-safety, low-cost, and long-life energy storage systems.

Author contributions

Z. J.: investigation, drawing, writing – original draft. M. X. & Q. M.: conceptualization, analysis. P. L.: conceptualization, supervision. H. Y.: writing – review & editing.

Conflicts of interest

There are no conflicts to declare.

Data availability

No primary research results, software or code have been included, and no new data were generated or analysed as part of this review.

Acknowledgements

The authors would like to extend their sincere thanks to Professor Yuejiao Chen at Central South University for her invaluable suggestion on the scope and structure of this review. This research did not receive any specific grant from funding agencies in the public, commercial, or not-for-profit sectors.

References

1 Y. Tang, J. Xie, Y. Chen, X. Liu and X. Kang, A Minireview on Comprehensive Application of Hydrogels Used as Electrolytes in Flexible Zinc-Air Batteries, *J. Polym. Mater.*, 2025, **42**, 587–619.
2 L. Canglong, Q. Hongli, H. Jie, C. Dongping, C. Yuanzi, X. Minghan, J. Zihao, Y. Huaming, H. Yang, L. Guanghui and C. Yuejiao, Enabling highly reversible Zn anode via an interfacial preferentially adsorbed additive containing nucleophilic groups, *Microstructures*, 2025, **5**, 2025033.
3 Y. Yang, C. Zhang, Z. Mei, Y. Sun, Q. An, Q. Jing, G. Zhao and H. Guo, Interfacial engineering of perfluoroalkyl functionalized covalent organic framework achieved ultra-long cycled and dendrite-free lithium anodes, *Nano Res.*, 2023, **16**, 9289–9298.
4 S. Kim, G. Park, S. J. Lee, S. Seo, K. Ryu, C. H. Kim and J. W. Choi, Lithium-Metal Batteries: From Fundamental Research to Industrialization, *Adv. Mater.*, 2023, **35**, e2206625.
5 Z. He, H. Yu, M. Fu, Q. Li, C. Li, T. Li, C. Zhang, Y. Chen and L. Chen, Competitive solvation with regulated ion-coordination chemistry toward dendrite-free and long-life Zn metal anodes, *Energy Storage Mater.*, 2024, **70**, 103469.
6 G. Behzadi pour and L. Fekri aval, Recent advances in supercapacitors based on MXene surface modification: A review of symmetric and asymmetric electrodes material, *Results Eng.*, 2024, **24**, 103045.
7 G. B. Pour, L. F. Aval and H. Nazarpour-Fard, Effectiveness of Nitrogen-Doping in MXene-Based Composites for Supercapacitor Electrodes, *Results Chem.*, 2025, **13**, 101965.
8 G. B. Pour and L. F. Aval, in *Supercapacitors: Fundamentals, Advances and Future Applications*, ed. D. K. Verma and J. Aslam, Royal Society of Chemistry, 2025, vol. 3, p. 128.
9 H. Lu, S. Meng, T. He, C. Zhang and J. Yang, Recent progress in covalent organic frameworks for rechargeable zinc-based batteries, *Coord. Chem. Rev.*, 2024, **514**, 215910.
10 M. Tang, Q. Liu, X. Zou, B. Zhang and L. An, High-Energy-Density Aqueous Zinc-Ion Batteries: Recent Progress, Design Strategies, Challenges, and Perspectives, *Adv. Mater.*, 2025, **1**, 2501361.
11 H. Gan, H. Zhang, S. Ying, J. Dong, J. Zhang, D. Li, Q. Huang, S. Zheng, C. Hu, Q. Sun, J. Ai, J. Wang and B. Zhou, A review of composite polymer electrolytes with fast lithium-ion conductors for rechargeable lithium batteries, *Chem. Eng. J.*, 2025, **522**, 167671.
12 S. Huang, S. Shi, H. Qi, L. Wang, Y. Zhao, C. Li, D. Chen, H. Yu, Y. Chen and L. Chen, Dual confinement of water and anions to stabilize zinc anode via a nanocluster colloidal electrolyte, *Appl. Surf. Sci.*, 2025, **710**, 163943.
13 X. Li, F. Luo, N. Zhou, H. Adenusi, S. Fang, F. Wu and S. Passerini, Weakly Solvating Electrolytes for Lithium and Post-Lithium Rechargeable Batteries: Progress and Outlook, *Adv. Energy Mater.*, 2025, **15**, 2501272.
14 K. Jin and Y. Yu, Principles, progress, and prospects of photo-rechargeable zinc-ion batteries, *J. Energy Chem.*, 2025, **104**, 382–396.
15 Z. Pei, Symmetric is nonidentical: Operation history matters for Zn metal anode, *Nano Res. Energy*, 2022, **1**, 9120023.
16 L. Li, S. Liu, J. Luo, X. Hou, J. Kong, Q. Zhang, W. Lai and C. He, Three-dimensional architecture design enables hexaazatriphenylene-based polymers as high-voltage, long-lifespan cathodes for aqueous zinc–organic batteries, *eScience*, 2025, **5**, 100379.
17 D. Wang, Q. Li, Y. Zhao, H. Hong, H. Li, Z. Huang, G. Liang, Q. Yang and C. Zhi, Insight on Organic Molecules in Aqueous Zn-Ion Batteries with an Emphasis on the Zn Anode Regulation, *Adv. Energy Mater.*, 2022, **12**, 2102707.
18 M. Wang, J. Ma, Y. Meng, J. Sun, Y. Yuan, M. Chuai, N. Chen, Y. Xu, X. Zheng, Z. Li and W. Chen, High-Capacity Zinc Anode with 96% Utilization Rate Enabled by Solvation Structure Design, *Angew. Chem., Int. Ed.*, 2023, **62**, e202214966.
19 J. Li, A. Azizi, S. Zhou, S. Liu, C. Han, Z. Chang, A. Pan and G. Cao, Hydrogel polymer electrolytes toward better zinc-ion batteries: A comprehensive review, *eScience*, 2025, **5**, 100294.
20 S. Huang, K. Li, Z. He, Y. Wang, C. Li, H. Li, H. Yu, Y. Chen and L. Chen, Rolling strategy for highly efficient preparation of phosphating interface enabled the stable lithium anode, *J. Alloys Compd.*, 2024, **1005**, 176193.
21 J. Yin, Y. Tan and J. Pu, Advanced electrolyte strategies for dendrite-free aqueous Zn–metal batteries, *Chem. Commun.*, 2025, **61**, 5857–5870.
22 P. A. Shinde, N. R. Chodankar, L. K. Shrestha, A. Al Ghaferi, E. Alhajri and K. Ariga, Stable and Dendrite-Free Zinc Metal Anodes Via Interface Nanoarchitectonics for Aqueous Zinc-Ion Batteries, *Adv. Funct. Mater.*, 2025, **1**, e2424242.
23 Z. Cao, P. Zhuang, X. Zhang, M. Ye, J. Shen and P. M. Ajayan, Strategies for Dendrite-Free Anode in Aqueous Rechargeable Zinc Ion Batteries, *Adv. Energy Mater.*, 2020, **10**, 2001599.

24 H. Ni, Z. Fan, J. Wang and Y. Wu, Research Progress on the Mechanisms of MOF/COF and Their Derivatives in Zinc–Ion Batteries, *Energy Storage Mater.*, 2025, **77**, 104220.
25 Y. A. Kumar, S. Vignesh, T. Ramachandran, K. D. Kumar, A. G. Al-Sehemi, M. Moniruzzaman and T. H. Oh, Solidifying the future: Metal-organic frameworks in zinc battery development, *J. Energy Storage*, 2024, **97**, 112826.
26 H. Lin, J. Yu, F. Chen, R. Li, B. Y. Xia and Z.-L. Xu, Visualizing the Interfacial Chemistry in Multivalent Metal Anodes by Transmission Electron Microscopy, *Small Methods*, 2023, **7**, 2300561.
27 W. Hu, X. Liu, Y. Pang, A. Li, Z. Lyu and Q. Li, A functional interlayer of PVDF-CTFE/MCA-HOFs for inhibiting zinc dendrite growth to improve the performance of aqueous zinc-ion batteries, *J. Alloys Compd.*, 2025, **1022**, 179843.
28 M. Wang, Y. Meng, X. Li, J. Qi, A. Li and S. Huang, Challenges and strategies for zinc anodes in aqueous Zinc-Ion batteries, *Chem. Eng. J.*, 2025, **507**, 160615.
29 Y. Zheng, J. Zheng and H. Liang, Polyacrylic Acid-Modified Gel Electrolytes for Enhanced Electrochemical Performance in Aqueous Zinc Batteries, *Batteries Supercaps*, 2025, **8**, e202400776.
30 M. K. Lee, M. Shokouhimehr, S. Y. Kim and H. W. Jang, Two-Dimensional Metal–Organic Frameworks and Covalent–Organic Frameworks for Electrocatalysis: Distinct Merits by the Reduced Dimension, *Adv. Energy Mater.*, 2022, **12**, 2003990.
31 M. Szwast and D. Polak, Hybrid MOF-COF structures for advanced gas separation membranes: a short review of synthesis, performance analysis and application potential, *Rev. Chem. Eng.*, 2025, **41**, 525–538.
32 Y. Zhang, S. Sun, M. Wang, Q. Shen, S. Cong, Y. Zhao, J. Peng and H. Pang, Metal-organic framework (MOF) membranes for Mg2+/Li+ separation, *Sep. Purif. Technol.*, 2025, **374**, 133737.
33 C. Wei, L. Tan, Y. Zhang, S. Xiong and J. Feng, Metal-organic frameworks and their derivatives in stable Zn metal anodes for aqueous Zn-ion batteries, *ChemPhysMater*, 2022, **1**, 252–263.
34 H. Hong, X. Guo, J. Zhu, Z. Wu, Q. Li and C. Zhi, Metal/covalent organic frameworks for aqueous rechargeable zinc-ion batteries, *Sci. China: Chem.*, 2024, **67**, 247–259.
35 A. Kausar, Covalent Organic Framework (COF)—Topical Game Changer for Polymeric Nanocomposites, *Polym.-Plast. Technol. Mater.*, 2025, **64**, 1947–1978.
36 M. Gopalakrishnan, S. Ganesan, M. T. Nguyen, T. Yonezawa, S. Praserthdam, R. Pornprasertsuk and S. Kheawhom, Critical roles of metal–organic frameworks in improving the Zn anode in aqueous zinc-ion batteries, *Chem. Eng. J.*, 2023, **457**, 141334.
37 Y. Wang, Y. Qi, G. Bi, W. Yin and W. Zhang, Temperature-Adaptive Aqueous Zinc–Iodine Batteries Enabled by Ionic Covalent Organic Framework Modified Separator, *J. Phys. Chem. Lett.*, 2025, **16**, 5515–5522.
38 P. Xue, C. Guo, L. Li, H. Li, D. Luo, L. Tan and Z. Chen, A MOF-Derivative Decorated Hierarchical Porous Host Enabling Ultrahigh Rates and Superior Long-Term Cycling of Dendrite-Free Zn Metal Anodes, *Adv. Mater.*, 2022, **34**, 2110047.
39 X. Pan, X. Liu and C. C. Li, Covalent organic framework-derived functional interphase for improving Zn chemistry in aqueous zinc-ion batteries, *J. Mater. Chem. A*, 2025, **13**, 26847–26866.
40 Y. Wang, T. Pan, S. Zhang, Q. Li and H. Pang, MOF-based electrode materials for aqueous zinc-ion batteries: design strategy and future challenges, *Inorg. Chem. Front.*, 2025, **12**, 2988–3017.
41 Y. Zhang, C. Wei, M.-X. Wu, Y. Wang, H. Jiang, G. Zhou, X. Tang and X. Liu, A high-performance COF-based aqueous zinc-bromine battery, *Chem. Eng. J.*, 2023, **451**, 138915.
42 E. M. Johnson, S. Ilic and A. J. Morris, Design Strategies for Enhanced Conductivity in Metal–Organic Frameworks, *ACS Cent. Sci.*, 2021, **7**, 445–453.
43 C. Yang, Y. Xiang and Y. Yu, Electronic Conductive Metal–Organic Frameworks for Aqueous Rechargeable Zinc-Ion Battery Cathodes: Design, Progress, and Prospects, *Carbon Energy*, 2025, **7**, e70012.
44 C. Li, J. Huang, D. Chen, J. Li, Y. Cheng, T. You, S. Huang, H. Yu, Y. Huang, G. Li and Y. Chen, Accelerating Desolvation Process and Achieving Dendrite-Free Zn Anode Via Dielectric Filler-assisted Artificial Hybrid Interphase, *Adv. Sustainable Syst.*, 2025, **9**, 2401048.
45 S.-J. Lee, J.-H. Choi, I. Hwang, M.-H. Ryu, K.-N. Jung, H.-G. Cho, J. In Lee and G. Park, Interfacial engineering with BN@cellulose separator to suppress dendrite growth and side reactions in aqueous zinc-ion batteries, *Electrochem. Commun.*, 2025, **172**, 107882.
46 H. Zhang, M. Zhang, T. Xu, X. Wang, J. Qi, Y. Wang, W. Liu, L. Zhu, Z. Yuan and C. Si, Ions and electrons dual transport channels regulated by nanocellulose for mitigating dendrite growth of zinc-ion batteries, *Chem. Eng. J.*, 2025, **505**, 159476.
47 M. Liu, L. Yang, H. Liu, A. Amine, Q. Zhao, Y. Song, J. Yang, K. Wang and F. Pan, Artificial Solid-Electrolyte Interface Facilitating Dendrite-Free Zinc Metal Anodes via Nanowetting Effect, *ACS Appl. Mater. Interfaces*, 2019, **11**, 32046–32051.
48 X. Xu, Y. Xu, J. Zhang, Y. Zhong, Z. Li, H. Qiu, H. B. Wu, J. Wang, X. Wang, C. Gu and J. Tu, Quasi-Solid Electrolyte Interphase Boosting Charge and Mass Transfer for Dendrite-Free Zinc Battery, *Nano-Micro Lett.*, 2023, **15**, 56.
49 K. Wu, X. Shi, F. Yu, H. Liu, Y. Zhang, M. Wu, H.-K. Liu, S.-X. Dou, Y. Wang and C. Wu, Molecularly engineered three-dimensional covalent organic framework protection films for highly stable zinc anodes in aqueous electrolyte, *Energy Storage Mater.*, 2022, **51**, 391–399.
50 R. Zhang, Y. Feng, Y. Ni, B. Zhong, M. Peng, T. Sun, S. Chen, H. Wang, Z. Tao and K. Zhang, Bifunctional Interphase with Target-Distributed Desolvation Sites and Directionally Depositional Ion Flux for Sustainable Zinc Anode, *Angew. Chem., Int. Ed.*, 2023, **62**, e202304503.

51 J. Zhao, Y. Ying, G. Wang, K. Hu, Y. D. Yuan, H. Ye, Z. Liu, J. Y. Lee and D. Zhao, Covalent organic framework film protected zinc anode for highly stable rechargeable aqueous zinc-ion batteries, *Energy Storage Mater.*, 2022, **48**, 82–89.
52 L. Lei, F. Chen, Y. Wu, J. Shen, X.-J. Wu, S. Wu and S. Yuan, Surface coatings of two-dimensional metal-organic framework nanosheets enable stable zinc anodes, *Sci. China: Chem.*, 2022, **65**, 2205–2213.
53 J. H. Park, M.-J. Kwak, C. Hwang, K.-N. Kang, N. Liu, J.-H. Jang and B. A. Grzybowski, Self-Assembling Films of Covalent Organic Frameworks Enable Long-Term, Efficient Cycling of Zinc-Ion Batteries, *Adv. Mater.*, 2021, **33**, 2101726.
54 L. Cao, D. Li, T. Deng, Q. Li and C. Wang, Hydrophobic Organic-Electrolyte-Protected Zinc Anodes for Aqueous Zinc Batteries, *Angew. Chem., Int. Ed.*, 2020, **59**, 19292–19296.
55 W. Xin, J. Xiao, J. Li, L. Zhang, H. Peng, Z. Yan and Z. Zhu, Metal-organic frameworks with carboxyl functionalized channels as multifunctional ion-conductive interphase for highly reversible Zn anode, *Energy Storage Mater.*, 2023, **56**, 76–86.
56 Y. Zhao, K. Feng and Y. Yu, A Review on Covalent Organic Frameworks as Artificial Interface Layers for Li and Zn Metal Anodes in Rechargeable Batteries, *Adv. Sci.*, 2024, **11**, 2308087.
57 Z. Zhao, R. Wang, C. Peng, W. Chen, T. Wu, B. Hu, W. Weng, Y. Yao, J. Zeng, Z. Chen, P. Liu, Y. Liu, G. Li, J. Guo, H. Lu and Z. Guo, Horizontally arranged zinc platelet electrodeposits modulated by fluorinated covalent organic framework film for high-rate and durable aqueous zinc ion batteries, *Nat. Commun.*, 2021, **12**, 6606.
58 S. H. Pang, C. Han, D. S. Sholl, C. W. Jones and R. P. Lively, Facet-Specific Stability of ZIF-8 in the Presence of Acid Gases Dissolved in Aqueous Solutions, *Chem. Mater.*, 2016, **28**, 6960–6967.
59 L. Lei, J. Dong, S. Ke, S. Wu and S. Yuan, Porous framework materials for stable Zn anodes in aqueous zinc-ion batteries, *Inorg. Chem. Front.*, 2023, **10**, 5555–5572.
60 H. Yang, Z. Chang, Y. Qiao, H. Deng, X. Mu, P. He and H. Zhou, Constructing a Super-Saturated Electrolyte Front Surface for Stable Rechargeable Aqueous Zinc Batteries, *Angew. Chem., Int. Ed.*, 2020, **59**, 9377–9381.
61 X. Zeng, J. Zhao, Z. Wan, W. Jiang, M. Ling, L. Yan and C. Liang, Controllably Electrodepositing ZIF-8 Protective Layer for Highly Reversible Zinc Anode with Ultralong Lifespan, *J. Phys. Chem. Lett.*, 2021, **12**, 9055–9059.
62 X. Suo, F. Zhang, Z. Yang, H. Chen, T. Wang, Z. Wang, T. Kobayashi, C.-L. Do-Thanh, D. Maltsev, Z. Liu and S. Dai, Highly Perfluorinated Covalent Triazine Frameworks Derived from a Low-Temperature Ionothermal Approach Towards Enhanced CO2 Electroreduction, *Angew. Chem., Int. Ed.*, 2021, **60**, 25688–25694.
63 X. Hu, Z. Lin, S. Wang, G. Zhang, S. Lin, T. Huang, R. Chen, L.-H. Chung and J. He, Highly Crystalline Flower-Like Covalent-Organic Frameworks Enable Highly Stable Zinc Metal Anodes, *ACS Appl. Energy Mater.*, 2022, **5**, 3715–3723.
64 D. Chen, P. Liu, L. Zhong, S. Wang, M. Xiao, D. Han, S. Huang and Y. Meng, Covalent Organic Frameworks with Low Surface Work Function Enabled Stable Lithium Anode, *Small*, 2021, **17**, 2101496.
65 C. Li, F. Liu, H. Yao, T. You, L. Wang, S. Huang, J. Huang, H. Wang, Y. Chen, L. Chen and G. Li, Dynamic pH Regulation and Interfacial Ion Redistribution via Molecular Buffering for Dendrite-Free Zn Metal Anodes, *Adv. Funct. Mater.*, 2025, e14260, DOI: 10.1002/adfm.202514260.
66 W. Cui, W. Jia, B. Yu, S. Wang, X. Zhang, X. Qubie, X. Lv and F. Wang, A Review on the Design of Cathode Catalyst Materials for Zinc-Iodine Batteries, *Catalysts*, 2025, **15**, 178.
67 L. Yang, J. Zhang, X. Zhou and Y. Liu, Amorphous aluminum-doped manganese oxide cathode with strengthened performance for aqueous zinc-ion batteries, *J. Alloys Compd.*, 2025, **1012**, 178502.
68 W. Zheng, Z.-H. Sun, Z.-Y. Gu, X.-L. Wu and L. Niu, Recent Advances in Vanadium-Based Cathode Materials for Aqueous Zinc-Ion Batteries: from Fundamentals to Practical Applications, *Adv. Mater. Technol.*, 2025, **10**, 2500320.
69 J. Sun, Y. Fei, H. Tang, J. Bao, Q. Zhang and X. Zhou, Covalent Organic Frameworks as Promising Electrode Materials for High-Valent Ion Rechargeable Batteries, *ACS Appl. Energy Mater.*, 2024, **7**, 7592–7602.
70 Q. Zhang, P. Zhi, J. Zhang, S. Duan, X. Yao, S. Liu, Z. Sun, S. C. Jun, N. Zhao, L. Dai, L. Wang, X. Wu, Z. He and Q. Zhang, Engineering Covalent Organic Frameworks Toward Advanced Zinc-Based Batteries, *Adv. Mater.*, 2024, **36**, 2313152.
71 Y. Kuai and Y. Wang, Innovative COF@MXene composites for high performance energy applications, *Carbon Neutrality*, 2024, **3**, 36.
72 K. A. Adegoke, K. G. Akpomie, E. S. Okeke, C. Olisah, A. Malloum, N. W. Maxakato, J. O. Ighalo, J. Conradie, C. R. Ohoro, J. F. Amaku and K. O. Oyedotun, UiO-66-based metal-organic frameworks for CO2 catalytic conversion, adsorption and separation, *Sep. Purif. Technol.*, 2024, **331**, 125456.
73 H. Zhang, M. Zhao and Y. S. Lin, Stability of ZIF-8 in water under ambient conditions, *Microporous Mesoporous Mater.*, 2019, **279**, 201–210.
74 S. Yuan, L. Feng, K. Wang, J. Pang, M. Bosch, C. Lollar, Y. Sun, J. Qin, X. Yang, P. Zhang, Q. Wang, L. Zou, Y. Zhang, L. Zhang, Y. Fang, J. Li and H.-C. Zhou, Stable Metal–Organic Frameworks: Design, Synthesis, and Applications, *Adv. Mater.*, 2018, **30**, 1704303.
75 Z. Wang, J. Hu, L. Han, Z. Wang, H. Wang, Q. Zhao, J. Liu and F. Pan, A MOF-based single-ion Zn2+ solid electrolyte leading to dendrite-free rechargeable Zn batteries, *Nano Energy*, 2019, **56**, 92–99.

76 C. Guo, J. Zhou, Y. Chen, H. Zhuang, J. Li, J. Huang, Y. Zhang, Y. Chen, S.-L. Li and Y.-Q. Lan, Integrated Micro Space Electrostatic Field in Aqueous Zn-Ion Battery: Scalable Electrospray Fabrication of Porous Crystalline Anode Coating, *Angew. Chem., Int. Ed.*, 2023, **62**, e202300125.

77 N. An, L. Liu, Y. Fang, L. Wang, C. Meng, D. Sun, J. He, L. Wang and Q. Wang, Porous covalent organic framework films with abundant zinc-philic groups by controlled interfacial polymerization for zinc anode protection, *J. Energy Storage*, 2025, **117**, 116214.

78 A. M. Khayum, M. Ghosh, V. Vijayakumar, A. Halder, M. Nurhuda, S. Kumar, M. Addicoat, S. Kurungot and R. Banerjee, Zinc ion interactions in a two-dimensional covalent organic framework based aqueous zinc ion battery, *Chem. Sci.*, 2019, **10**, 8889–8894.

79 D. Ma, H. Zhao, F. Cao, H. Zhao, J. Li, L. Wang and K. Liu, A carbonyl-rich covalent organic framework as a high-performance cathode material for aqueous rechargeable zinc-ion batteries, *Chem. Sci.*, 2022, **13**, 2385–2390.

80 L. Li, R. Bu, W. Zhong, Q. Wu, F. Wang, Z. Shen, S. Mao, J. Zhang, C. Tan, S. Zhang, B. Zhang, H. Gao, Y. Kim, Y. Lu and H. Cheng, Densely packed and vertically oriented covalent organic framework membrane enabled efficient ion sieving for zinc iodine battery, *Nano Energy*, 2025, **138**, 110886.

81 L. Yang, Q. Ma, Y. Yin, D. Luo, Y. Shen, H. Dou, N. Zhu, R. Feng, Y. Kong, A. Yu, B. Cheng, X. Wang and Z. Chen, Construction of desolvated ionic COF artificial SEI layer stabilized Zn metal anode by *in situ* electrophoretic deposition, *Nano Energy*, 2023, **117**, 108799.

82 C. Guo, J. Zhou, Y. Chen, H. Zhuang, Q. Li, J. Li, X. Tian, Y. Zhang, X. Yao, Y. Chen, S.-L. Li and Y.-Q. Lan, Synergistic Manipulation of Hydrogen Evolution and Zinc Ion Flux in Metal-Covalent Organic Frameworks for Dendrite-free Zn-based Aqueous Batteries, *Angew. Chem., Int. Ed.*, 2022, **61**, e202210871.

83 P. He, B. Li, B. Wang, D. Xie, K. Wang and W. Ai, Regulating Zn Deposition via Honeycomb-like Covalent Organic Frameworks for Stable Zn Metal Anodes, *ACS Appl. Mater. Interfaces*, 2025, **17**, 2556–2565.

84 H. Yu, X. Zhang, Y. Wang, M. Li, W. Chen, Z. Hu, M. Zhu and Y. Huang, Activation and Stabilization Strategies of Aluminum Metal Anode Toward High Performance Aqueous Al Metal Batteries, *Adv. Mater.*, 2025, **37**, e2507164.

85 W. Zhang, W. Qi, K. Yang, Y. Hu, F. Jiang, W. Liu, L. Du, Z. Yan and J. Sun, Boosting tough metal Zn anode by MOF layer for high-performance zinc-ion batteries, *Energy Storage Mater.*, 2024, **71**, 103616.

86 S. Liu, M. Maisuradze, M. Li, Q. Li, N. Kazemi and M. Giorgetti, Zincophilic MOF Protective Layer for Stable Zinc Anodes in Zinc-Ion Batteries, *Chem. – Eur. J.*, 2025, **1**, e02217.

87 D. Wang, S. Hu, T. Li, C. Chang, S. Li, S. Guo, H. Li, Q. Liu, J. Gong, J. Zhou and C. Han, Anti-dendrite separator interlayer enabling staged zinc deposition for enhanced cycling stability of aqueous zinc batteries, *Nat. Commun.*, 2025, **16**, 259.

88 H. Luo, H.-J. Zhang, Y. Tao, W. Yao and Y. Xue, Advances in manganese-based cathode electrodes for aqueous zinc-ion batteries, *Front. Energy*, 2025, **19**, 260–282.

89 H. Ye, X. Zeng, X. Li, K. He, Y. Li and Y. Yuan, Review of ion doping and intercalation strategies for advancing manganese-based oxide cathodes in aqueous zinc-ion batteries, *Nano Energy*, 2025, **136**, 110740.

90 Q. Ma, J. Chen, Y. Chen, Y. Li, Q. Wu, B. Sun, B. Guo, Y. Yuan, W. Liao, S. Wang, Z. Ma and B. Yu, A review of energy storage mechanisms, modification strategies, and commercialization prospects of manganese dioxide cathodes in zinc-ion batteries, *J. Energy Storage*, 2025, **132**, 117869.

91 H. Shi, H. Fu, G. Xue, Y. Lian, J. Zhao and H. Zhang, Progress of vanadium-based oxides as cathode materials for aqueous zinc-ion batteries, *Coord. Chem. Rev.*, 2025, **545**, 216984.

92 M. Zhao and X. Wu, Recent Progress on the Intercalation Strategies of Vanadium-Based Material Cathodes for Aqueous Zinc-Ion Batteries, *Chem. Rec.*, 2025, **1**, e202500194.

93 L. Long, K. Mei, Z. Hou, Y. Wang, H. Zhang and W. Sun, Organic small-molecule cathodes for aqueous zinc-ion batteries: design strategy, application and mechanism, *Nanoscale Horiz.*, 2025, **10**, 2340–2364.

94 W. Chen, T. Chen and J. Fu, Pivotal Role of Organic Materials in Aqueous Zinc-Based Batteries: Regulating Cathode, Anode, Electrolyte, and Separator, *Adv. Funct. Mater.*, 2024, **34**, 2308015.

95 J. Lee, I. Choi, E. Kim, J. Park and K. W. Nam, Metal-organic frameworks for high-performance cathodes in batteries, *iScience*, 2024, **27**, 110211.

96 S. Mondal, P. Samanta, R. Sahoo, T. Kuila and M. C. Das, Porous and chemically robust MIL-100(V) MOF as an efficient cathode material for zinc-ion batteries, *Chem. Eng. J.*, 2023, **470**, 144340.

97 K. W. Nam, S. S. Park, R. dos Reis, V. P. Dravid, H. Kim, C. A. Mirkin and J. F. Stoddart, Conductive 2D metal-organic framework for high-performance cathodes in aqueous rechargeable zinc batteries, *Nat. Commun.*, 2019, **10**, 4948.

98 Y. Ru, S. Zheng, H. Xue and H. Pang, Layered V-MOF nanorods for rechargeable aqueous zinc-ion batteries, *Mater. Today Chem.*, 2021, **21**, 100513.

99 X. Pu, B. Jiang, X. Wang, W. Liu, L. Dong, F. Kang and C. Xu, High-Performance Aqueous Zinc-Ion Batteries Realized by MOF Materials, *Nano-Micro Lett.*, 2020, **12**, 152.

100 H. Wu, S. Li, Y. Liu and Y. Shi, Self-assembled Zn-Co MOF nanospheres/rGO as cathode material for an asymmetric supercapacitor with high energy density, *Electrochim. Acta*, 2023, **462**, 142740.

101 M. M. Mohamed, A. Hussain, Y. P. Hardianto, M. Faheem, A. A. Mirghni, A. Helal and M. A. Aziz, Synergistic Role of UiO-66 and UiO-67 MOF-Modified Glass Fiber Separators for Dendrite-Free and Long-Life Zinc-Ion Batteries, *Asian J. Org. Chem.*, 2025, **14**, e202500204.
102 N. Maeboonruan, J. Lohitkarn, C. Poochai, A. Tuantranont, P. Limthongkul and C. Sriprachuabwong, Dendrite-free anodes enabled by MOF-808 and ZIF-8 modified glass microfiber separator for ultralong-life zinc-ion hybrid capacitors, *J. Energy Storage*, 2024, **85**, 111063.
103 X. Liu, Z. Han, S. Zhao, H. Tang, T. Tian, Q. Weng, X. Liu and T. Liu, A HKUST-1 coating with copper metal active site enables stabilized zinc metal anode, *Mater. Today Energy*, 2024, **44**, 101659.
104 T. Zhao, S. Peng, J. Yu, J. Chen, F. Luo, K. K. Lim, H. Hamsan and N. S. Nazri, Study on the effect of different shapes of HKUST-1 based cellulose battery separators on the performance of zinc batteries, *J. Energy Storage*, 2025, **133**, 118066.
105 X. Gong, J. Wang, Y. Shi, Q. Zhang, W. Liu, S. Wang, J. Tian and G. Wang, Inhibiting dendrites on Zn anode by ZIF-8 as solid electrolyte additive for aqueous zinc ion battery, *Colloids Surf., A*, 2023, **656**, 130255.
106 Q. Li, M. Bai, X. Wang, J. Li, X. Lin, S. Shao, D. Li and Z. Wang, A MOF@ZnIn2S4 Composite Quasi-Solid Electrolyte for Highly Reversible Zn-Ion Batteries, *Adv. Funct. Mater.*, 2025, **35**, 2502344.
107 B. Li, P. Ruan, X. Xu, Z. He, X. Zhu, L. Pan, Z. Peng, Y. Liu, P. Zhou, B. Lu, L. Dai and J. Zhou, Covalent Organic Framework with 3D Ordered Channel and Multi-Functional Groups Endows Zn Anode with Superior Stability, *Nano-Micro Lett.*, 2024, **16**, 76.
108 Z. Lin, L. Lin, J. Zhu, W. Wu, X. Yang and X. Sun, An Anti-Aromatic Covalent Organic Framework Cathode with Dual-Redox Centers for Rechargeable Aqueous Zinc Batteries, *ACS Appl. Mater. Interfaces*, 2022, **14**, 38689–38695.
109 S. Park, I. Kristanto, G. Y. Jung, D. B. Ahn, K. Jeong, S. K. Kwak and S.-Y. Lee, A single-ion conducting covalent organic framework for aqueous rechargeable Zn-ion batteries, *Chem. Sci.*, 2020, **11**, 11692–11698.
110 T. Qiu, T. Wang, W. Tang, Y. Li, Y. Li, X. Lang, Q. Jiang and H. Tan, Rapidly Synthesized Single-Ion Conductive Hydrogel Electrolyte for High-Performance Quasi-Solid-State Zinc-ion Batteries, *Angew. Chem.,– Int. Ed.*, 2023, **62**, e202312020.
111 H.-M. Yu, D.-P. Chen, L.-J. Zhang, S.-Z. Huang, L.-J. Zhou, G.-C. Kuang, W.-F. Wei, L.-B. Chen and Y.-J. Chen, Electrolyte engineering for optimizing anode/electrolyte interface towards superior aqueous zinc-ion batteries: A review, *Trans. Nonferrous Met. Soc. China*, 2024, **34**, 3118–3150.
112 J. Li, J. Qiao and K. Lian, Hydroxide ion conducting polymer electrolytes and their applications in solid supercapacitors: A review, *Energy Storage Mater.*, 2020, **24**, 6–21.